

# Characterising EGFR tyrosine kinase inhibitor-adapted non-small cell lung cancer cell lines



Thesis submitted by Timo Leopold Kuerten

MSc by Research (Cell Biology)

2019

Supervisors:

Prof. Martin Michaelis, Dr Mark Wass

School of Biosciences

Faculty of Science

University of Kent

## Declaration

No part of this thesis has been submitted in support of an application for any degree or qualification of the University of Kent or any other university or institute of learning.

A handwritten signature in black ink, appearing to read 'timo kuerten'.

Timo Leopold Kuerten

## **Acknowledgements**

First and foremost I would like to thank my supervisors Prof. Martin Michaelis and Dr Mark Wass for their help and advice throughout this project, especially with regards to Prof. Michaelis' valuable guidance and feedback for completion of this thesis. I would also like to thank Tharsagini for her valuable training and insights into this project and Edith for her continued support in the lab, without which this project would not have been able to progress.

I am also grateful to Eithaar, Helen, Jo, Dan, Nathan, Jasmine, Nova, Tash and Dunishiya for their help, advice and moral support – your company has been wonderful and I could not have asked for better labmates. I will miss you all and wish you the best of luck for the future!

Finally, I would like to thank my parents for their unconditional love and support, I would not have been able to achieve anything I have so far without your continued belief in me!

## Table of Contents

<b>Declaration .....</b>	<b>2</b>
<b>Acknowledgements.....</b>	<b>3</b>
<b>Abbreviations .....</b>	<b>6</b>
<b>List of figures .....</b>	<b>8</b>
<b>Abstract.....</b>	<b>9</b>
<b>1.0. Introduction .....</b>	<b>10</b>
1.0. Non-small cell lung cancer .....	10
1.1. Targeted therapies for treating NSCLC .....	11
1.2. Epidermal Growth Factor Receptor (EGFR) signalling and an introduction to EGFR Tyrosine Kinase Inhibitors (TKIs).....	12
1.3. Overview of acquired drug resistance in cancer.....	14
1.4. Development and evolution of EGFR tyrosine kinase inhibitors .....	15
1.4.1. First generation EGFR tyrosine kinase inhibitors .....	15
1.4.2. Second generation EGFR tyrosine kinase inhibitors .....	16
1.4.3. Third generation EGFR tyrosine kinase inhibitors.....	17
1.5. Other resistance mechanisms.....	18
1.5.1. Alternate signalling pathway activation.....	18
1.5.2. Metabolic changes arising in resistance .....	22
1.6. Project aims and objectives .....	23
<b>2.0. Materials and Methods .....</b>	<b>24</b>
2.1. Cell lines .....	24
2.2. Cell culture .....	24
2.3. xCELLigence growth assay.....	25
2.4. SRB assay.....	25
<b>3.0. Results.....</b>	<b>27</b>
3.1. Morphological and growth characterisation of parental and resistant cell lines.....	28
3.2. IC50 characterisation of parental and resistant cell lines.....	35
<b>4.0. Discussion.....</b>	<b>51</b>
4.1. Resistance affects cell growth and morphology .....	51
4.2. EGFR TKI resistance leads to cross-resistance to paclitaxel treatment in multiple HCC827 and HCC4006 resistant sub-lines.....	53
4.3. A possible shift to MET signalling may affect the response of resistant HCC827 and HCC4006 cell lines to osimertinib and cabozantinib .....	54
4.4. Sensitivity to MEK inhibition emerges in EGFR TKI resistant HCC827 but not HCC4006 cells .....	55
4.5. Sensitivity to cabozantinib emerges in resistant HCC827 and HCC4006 cell lines .....	57

4.6.	EGFR TKI resistant cell lines show no increased sensitivity to dichloroacetate .....	58
4.7.	Future work.....	59
4.8.	Conclusions .....	61
	<b>Bibliography .....</b>	<b>63</b>

## Abbreviations

nM	Nanomolar
$\mu$ M	Micromolar
mM	Millimolar
ABCB1	ATP-binding cassette, sub-family B member 1
ABCG1	ATP binding cassette, sub-family G member 1
AKT	Protein kinase B
ATP	Adenosine triphosphate
CFDA	China Food and Drug Administration
c-SRC	Cellular Src kinase
DCA	Dichloroacetate
EDTA	Ethylenediaminetetraacetic acid
EGF	Epidermal growth factor
EGFR	Epidermal growth factor receptor
EMA	European Medicines Agency
EMT	Epithelial to mesenchymal transition
ERK	Extracellular signal-regulated kinase
FBS	Foetal bovine serum
FDA	Food and Drugs Administration (U.S.A)
HER	Human epidermal growth factor receptor
HGF	Hepatocyte growth factor
IC50	Inhibitory concentration (50%)
IMDM	Iscoe's modified Dulbecco's medium
MAPK	Mitogen-activated protein kinase
mTORC 1	Mammalian target of rapamycin complex 1
ncRNA	non-coding RNA
NGS	Next-generation sequencing
NSCLC	Non-small cell lung cancer
OS	Overall survival
PFS	Progression-free survival
PBS	Phosphate buffered saline

PDK	Pyruvate dehydrogenase kinase
PI3K	Phosphoinositide 3-kinase
RTCA	Real-time cell analysis
RTK	Receptor tyrosine kinase
RAF	Rapidly accelerated fibrosarcoma
SOS	Son of Sevenless
SP	Side population
SRB	Sulforhodamine B
TCA	Trichloroacetic acid
TKI	Tyrosine kinase inhibitor

## List of figures

- Figure 1.1** Simplified diagram of EGFR signalling
- Figure 1.2** An overview of factors contributing to acquired resistance in cancer
- Figure 1.3** Simplified diagram of MET and EGFR pathway crosstalk
- Figure 2.1** 96-well plate layout of SRB assay
- Figure 3.1** Figure 3.1 Brightfield microscopy of HCC827 sub-lines in culture
- Figure 3.2** Brightfield microscopy of HCC4006 sub-lines in culture
- Figure 3.3** Figure 3.3 Growth curves and doubling times of HCC827 and HCC4006 sub-lines
- Figure 3.4** Dose-response curves of HCC827 PTL cells treated with anti-cancer drug panel
- Figure 3.5** Dose-response curves of HCC827 rErlo cells treated with anti-cancer drug panel
- Figure 3.6** Dose-response curves of HCC827 rGefi cells treated with anti-cancer drug panel
- Figure 3.7** Dose-response curves of HCC827 rAfa cells treated with anti-cancer drug panel
- Figure 3.8** Dose-response curves of HCC4006 PTL cells treated with anti-cancer drug panel
- Figure 3.9** Dose-response curves of HCC4006 rErlo cells treated with anti-cancer drug panel
- Figure 3.10** Dose-response curves of HCC4006 rGefi cells treated with anti-cancer drug panel
- Figure 3.11** Dose-response curves of HCC4006 rAfa cells treated with anti-cancer drug panel
- Figure 3.12** IC50 comparison of HCC827 sub-lines treated with anti-cancer drug panel
- Figure 3.13** IC50 comparison of HCC4006 sub-lines treated with anti-cancer drug panel



## **Abstract**

Tyrosine kinase inhibitors (TKIs) that target the human epidermal growth factor receptor (EGFR) are targeted therapies used in the clinic for treating non-small cell lung cancer (NSCLC) harbouring activating mutations in the EGFR protein. As a targeted therapy, EGFR TKIs offer several benefits over broad-spectrum general chemotherapy, mainly through increased efficacy and a reduction in adverse side effects.

However, acquired drug resistance to EGFR TKIs is a pervasive issue, leading to the development of several generations of these drugs in an attempt to overcome it.

Unfortunately, due to a variety of distinct mechanisms, acquired resistance inevitably manifests itself after treatment with each new generation of inhibitors. The aim of this project was therefore to characterise HCC827 and HCC4006 NSCLC cell lines that had each been drug-adapted to erlotinib, gefitinib or afatinib by examining their morphology, growth and response to a drug panel comprised of 5 anti-cancer drugs with varying mechanisms of action – paclitaxel, osimertinib, trametinib, cabozantinib and dichloroacetate.

The characterisation process highlighted the strong heterogeneity associated with acquired drug resistance – despite being derived from the same tissue and NSCLC subtype (adenocarcinoma) as well as harbouring very similar EGFR-activating mutations, the morphology, growth and drug response rates between HCC827 and HCC4006 cells adapted to the same EGFR TKI showed a high degree of variability, with cross-resistance arising in at least one resistant sub-line for each drug. The most effective drug at overcoming acquired resistance was cabozantinib, with 3 out of 6 resistant sub-lines showing significantly decreased IC<sub>50</sub> when treated with the drug compared to the parental cells.

## **1.0. Introduction**

### **1.0. Non-small cell lung cancer**

One in two people born in the United Kingdom after 1960 will be diagnosed with cancer at some point in their life<sup>1</sup>. In essence, cancer is the transformation of healthy cells into malignant cells with unregulated cell division, which can then invade other tissues. In fact, there are over 100 different types of cancer, being differentiated based on tissue of origin as well as cancer subtype<sup>2</sup>. This is important as it means that each cancer type will have distinct oncogenic drivers and a unique response to anti-cancer treatments<sup>3</sup>.

Of these 100+ types, 13% of the people diagnosed with cancer will be diagnosed with lung cancer, making it the third most common cancer in the UK, and the most common worldwide. It is also the cancer with the highest mortality rate in the UK, accounting for 21% of all cancer deaths<sup>1</sup>.

Non-small cell lung cancer (NSCLC), which includes squamous cell carcinoma, adenocarcinoma and large cell carcinoma subtypes, accounts for 87% of lung cancers, and 49-53% of NSCLCs are diagnosed at stage IV. At this point, surgery ceases to be an option for most patients due to the cancer metastasising to other sites outside of the lung, meaning that it is no longer possible to excise all the tumours<sup>1</sup>. This makes drug therapy one of the only treatment options, although the current 5 year survival rate of patients with stage IV NSCLC is under 10%<sup>4</sup>. This highlights an urgent need for drug therapies that can effectively treat NSCLC in these patients.

### **1.1. Targeted therapies for treating NSCLC**

Whilst general broad-spectrum chemotherapy agents (such as cisplatin, carboplatin, gemcitabine, paclitaxel, among others<sup>5</sup>) were the default treatment option for non-small cell lung cancer for decades, they provide limited efficacy and lead to a plethora of adverse side effects including strong nausea, fevers, myelosuppression and may also result in neurotoxicity, nephrotoxicity and ototoxicity<sup>5,6</sup>. However targeted therapies, the principle of which is to target a specific oncogenic driver, often result in fewer and less uncomfortable side effects. The first FDA-approved targeted therapies for NSCLC were EGFR tyrosine kinase inhibitors (TKIs) gefitinib (2003)<sup>7</sup> and erlotinib (2004)<sup>8</sup>.

## 1.2. Epidermal Growth Factor Receptor (EGFR) signalling and an introduction to EGFR Tyrosine Kinase Inhibitors (TKIs)

EGFR tyrosine kinase inhibitors (TKIs) are a class of small-molecule drugs that target the epidermal growth factor receptor (EGFR), a member of the HER receptor tyrosine kinase (RTK) family. Under normal conditions the EGFR receptor plays an important part in regulating cell growth, proliferation, migration and differentiation by dimerising either with itself or with other members of the HER family when stimulated by bound epidermal growth factor (EGF), resulting in signal transduction and thus activation of proliferation and survival pathways<sup>9</sup>.

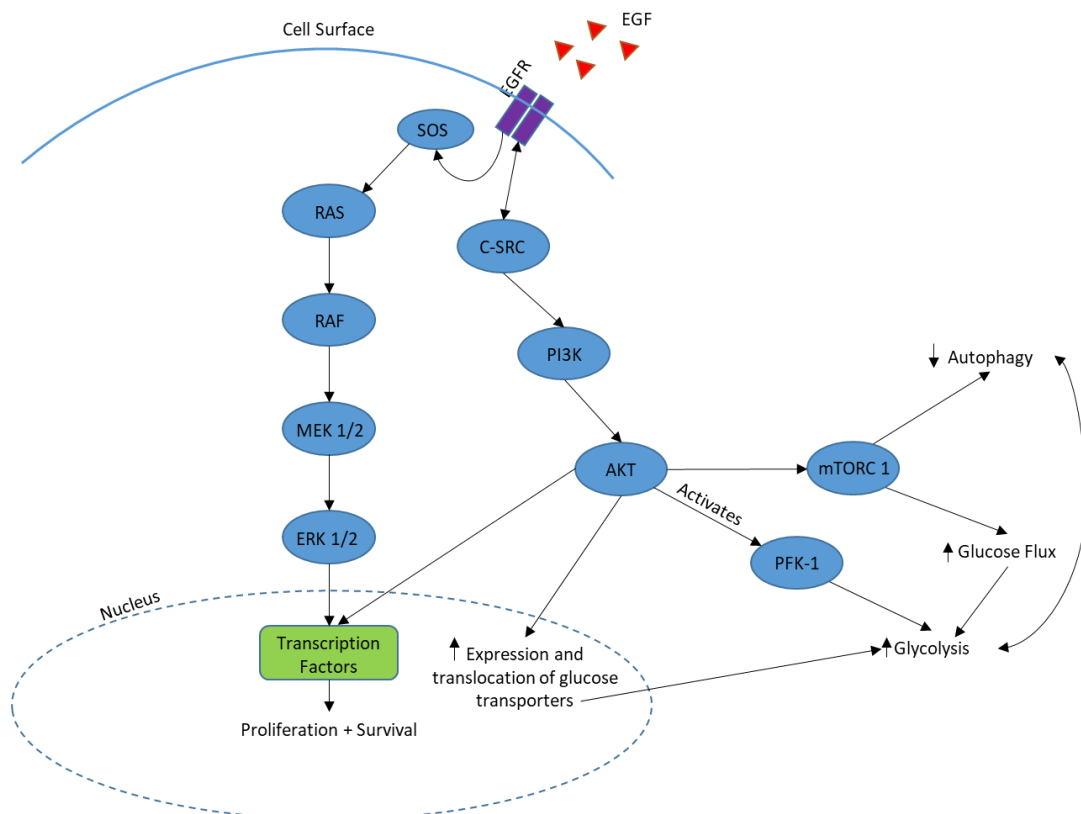


Figure 1.1 Simplified diagram of EGFR signalling.

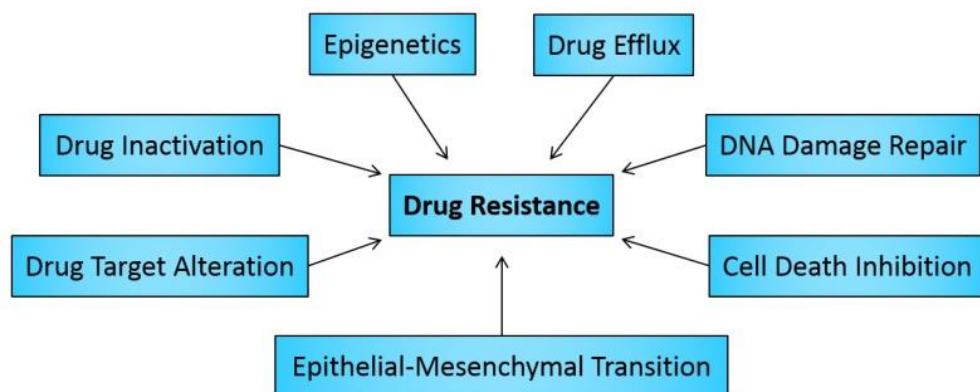
However, in NSCLC, around 24% of patients harbour tumours containing activating mutations in their EGFR proteins, causing it to become constitutively active<sup>10</sup>. Because this activating mutation is the main driver behind the carcinogenesis (also known as “oncogene addiction”) in these cells, they are sensitive to EGFR TKIs.

The most common EGFR activating mutations in NSCLC, responsible for 85-90% of mutations, are an exon 19 deletion resulting in the loss of a leucine-arginine-glutamate-alanine motif in the tyrosine kinase domain of the receptor, and a transversion in exon 21 that results in a leucine to arginine substitution at position 858 (L858R), also in the tyrosine kinase domain<sup>10</sup>. These mutations enable the receptor to undergo ligand-independent dimerization, leading to constitutively active signalling<sup>11</sup>. Both of these mutations affect the conformation of the receptor’s ATP binding pocket, resulting in decreased affinity for ATP and a heightened affinity for EGFR TKIs when compared to the wild-type receptor<sup>12</sup>.

EGFR TKIs demonstrate increased efficacy in patients with exon 19 deletions and L858R substitutions compared to classical chemotherapy, with median overall survival being 20 months for patients treated with Erlotinib or Gefitinib<sup>10</sup> compared to a median overall survival of 7.8 months for the reference chemotherapy treatment of cisplatin and paclitaxel<sup>13</sup>.

### 1.3. Overview of acquired drug resistance in cancer

One of the greatest setbacks in treating non-small cell lung cancer is the development of acquired drug resistance, which arises after initial treatment response; if the tumour is insensitive to the drug from the very onset of the treatment course then this is known as intrinsic resistance, which is outside the scope of this project. As a basic concept, acquired resistance can be defined as the “phenomenon that results when (cancers) become tolerant to pharmaceutical treatments<sup>14</sup>.” However, the aetiology of acquired resistance in the context of cancer is significantly more complex and relies on a series of often-overlapping factors. The most well-studied of these mechanisms include epigenetic changes, drug efflux, DNA damage repair, cell death inhibition, epithelial-mesenchymal transition (EMT), drug target alteration and drug inactivation<sup>14</sup> although other factors such as non-coding RNAs (ncRNA), which can modulate and interact with the more classical resistance mechanisms are beginning to be uncovered and investigated in more detail<sup>15</sup>.



**Figure 1.2 An overview of factors contributing to acquired resistance in cancer.** Adapted from Housman et al. (2014) “Drug Resistance in Cancer: An Overview”

In the context of NSCLC treatment with EGFR inhibitors, the most common of these factors is drug target alteration through various different mechanisms, as discussed below.

#### **1.4. Development and evolution of EGFR tyrosine kinase inhibitors**

As with many targeted therapies, drug resistance is a major problem for EGFR TKIs. The most common mechanism of acquired resistance in NSCLC (50-60% of cases of resistance) is through a secondary gatekeeper mutation in the tyrosine kinase domain at amino acid 790, known as a T790M mutation<sup>16</sup> caused by a C>T substitution at position 2369 in the EGFR gene<sup>17</sup>. This has led to multiple generations of EGFR TKIs being developed in an attempt to overcome common resistance mechanisms, with the most recent attempt being third-generation EGFR TKIs.

##### **1.4.1. First generation EGFR tyrosine kinase inhibitors**

As the name suggests, first-generation EGFR inhibitors were the first to be developed. These drugs bind reversibly to the ATP binding pocket in EGFR with the aforementioned activating mutations. The most well-known examples are erlotinib and gefitinib, which have both been approved for use in NSCLC by the FDA and the EMA, whilst icotinib has been approved by China's CFDA<sup>18</sup>. While initial response rates to first generation EGFR inhibitors in patients with the exon 19 deletion or L858R substitutions are high, acquired resistance to the drugs rapidly develops. There are various mechanisms which can mediate this resistance such as BRAF and PI3K mutations, as well as MET amplifications. However, the most common is a substitution from a threonine to a methionine at position 790, also known as a T790M mutation and is found in over 50% of patients treated with first generation EGFR inhibitors who have developed resistance<sup>16</sup>. There are two main molecular mechanisms describing

how the T790M mutation results in resistance. First, the change from a threonine to a methionine residue with a larger sidechain results in a conformational change in the ATP binding pocket, decreasing its affinity for first generation EGFR TKIs<sup>19</sup>. Secondly, specifically in tumours containing the L858R activating mutation, the substitution causes the ATP binding pocket to regain affinity for ATP, bringing it up to near wild-type EGFR levels and thus decreasing the site's affinity for the drugs<sup>20</sup>.

#### **1.4.2. Second generation EGFR tyrosine kinase inhibitors**

Second generation EGFR TKIs were designed as a response to the rapidly acquired resistance of NSCLC to first-generation drugs. They bind irreversibly to the ATP binding pocket, which was postulated to increase sensitivity in T790M mutated tumours as the irreversible binding would allow them to overcome the restored affinity to ATP found in T790M mutated cells<sup>21</sup>. This also meant, however, that their specificity for the mutant EGFR was reduced, with increased binding to the wild-type receptor compared to first generation inhibitors<sup>22</sup>. FDA and EMA-approved 2<sup>nd</sup> generation therapies include afatinib and dacomitinib, which were shown to be effective against cells containing T790M mutations *in vitro*, but were not able to reach the required concentration to achieve this effect in clinical trials. Treatment with afatinib after a course of first-generation EGFR TKIs showed an increase in progression free survival (PFS) but not overall survival (OS) when compared to a placebo<sup>23</sup>. Second generation EGFR TKIs may thus be better suited as a first-line therapy, as both afatinib and dacomitinib show an increase in PFS when compared directly to first-generation EGFR TKIs.<sup>24,25</sup> Overall, this demonstrates that second-generation EGFR inhibitors did not have the desired effectiveness against patients with T790M mutated tumours, which in turn led to the development of third-generation EGFR TKIs.



### 1.4.3. Third generation EGFR tyrosine kinase inhibitors

A second attempt to effectively tackle the acquired T790M mutation, third generation EGFR TKIs also bind irreversibly to the ATP binding pocket in EGFR. Osimertinib is currently the only FDA and EMA approved third-generation EGFR inhibitor, so that is the drug that will be focussed on in this context. In contrast to second generation inhibitors, it has almost 200 times more potency against the two common mutant EGFR types compared to the wild-type receptor<sup>26</sup>. Its chemical design allows it to overcome the common T790M resistance mutation, with clinical trials showing that it is more effective than platinum doublet chemotherapy (10.1 months PFS with osimertinib compared to 4.4 months with platinum therapy plus pemetrexed)<sup>27</sup> at treating patients with T790M mutations, making it an effective second-line therapy once resistance to first or second generation inhibitors develops. Interestingly, it was also demonstrated to be more effective than first generation inhibitors in treatment-naïve patients with activating mutations, showing a median PFS of 18.9 months for osimertinib compared to 10.2 months for first generation TKIs<sup>28</sup>. Despite its effectiveness at overcoming the T790M mutation, osimertinib is itself unfortunately not immune to the generation of resistance. C797S, a tertiary mutation in EGFR caused by a T>A substitution at position 2398<sup>29</sup>, is one of the most common mechanisms of resistance to third-generation inhibitors. By changing the conformation of the binding pocket once again through this substitution, the drug can no longer bind effectively and the therapeutic effect diminishes<sup>30</sup>. Other mechanisms include alternate pathway activations such as c-MET amplification<sup>30</sup> and increased RAS signalling<sup>31</sup>.

## **1.5. Other resistance mechanisms**

Although the T790M mutation is the most common, there are also other mechanisms of resistance to EGFR inhibitors, such as bypass/alternative pathway activation (1-25% of cases), histological/phenotypic transformation (5-10%) or unknown causes (20-30%)<sup>30</sup>. Metabolic shifts caused by exposure to the drugs can also affect resistance, although this appears to be a co-factor more than an individual driver thereof. As they are the most common and easy to target (respectively) alternative mechanisms, the focus here will primarily be on alternative pathway activation and metabolic shift.

### **1.5.1. Alternate signalling pathway activation**

The most common pathway bypass leading to drug resistance in NSCLC is an amplification of MET receptor tyrosine kinase expression. There is significant cross-talk between the EGFR and MET receptors, as both feed into the MAPK and PI3K signalling pathways. In cases where MET amplification is the driver for resistance, a sub-population of NSCLC tumour cells have developed pre-existing MET amplification and are thus not oncogene-addicted to EGFR, limiting the effect of mono-target EGFR inhibitors as the MAPK and PI3K signalling pathways remain active to drive cell proliferation and survival<sup>32</sup>.

One possible option in the treatment of MET amplified, EGFR TKI resistant NSCLC is the use of MET inhibitors. If the tumour cells have abrogated EGFR signalling after treatment and are now reliant on MET signalling to drive tumourigenesis, then inhibiting its source should stop disease progression. MET inhibitors are similar to EGFR inhibitors in that they are small-molecule targeted inhibitors, however their mechanism of action varies according to the class of the MET inhibitor; some are ATP

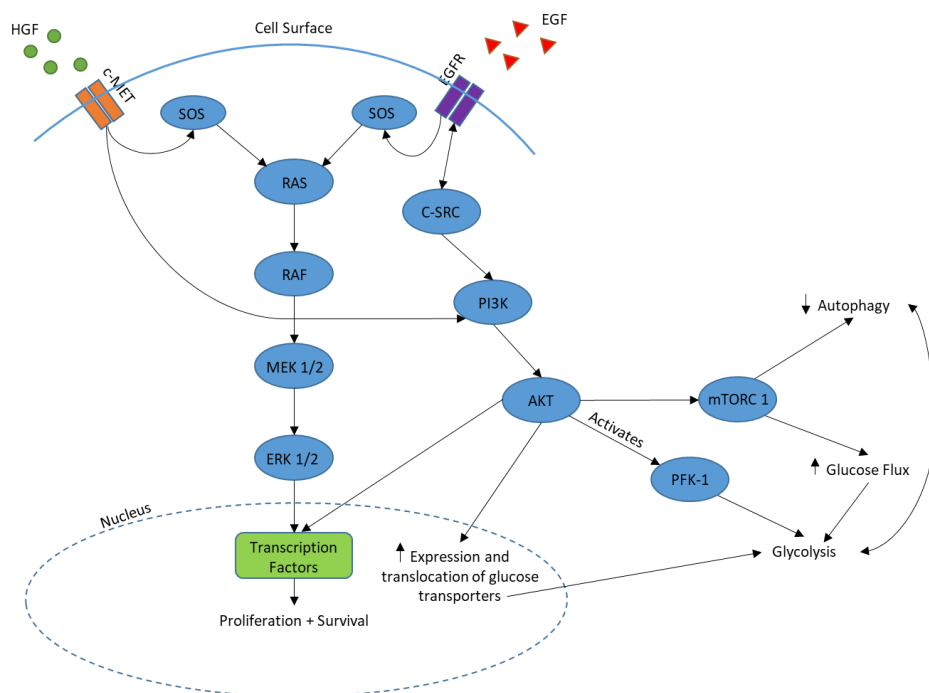
non-competitive whereas others are ATP competitive<sup>33</sup>. ATP competitive MET inhibitors can further be classed into two sub-types: type I inhibitors are highly specific to MET, whereas type II inhibitors have broader-spectrum TKI effects and often inhibit other receptor tyrosine kinases to varying degrees<sup>34,35</sup>.

Cabozantinib is an ATP-competitive type II inhibitor and was originally developed to treat medullary thyroid cancer<sup>33</sup>. It has a high affinity for MET but also demonstrates activity against VEGFR2, ROS, KIT, RET, AXL, RON, FLT3 and TIE-2 RTKs to different extents<sup>35</sup>. MET, VEGFR, ROS, RET and AXL are implicated in lung cancer tumorigenesis<sup>36</sup>, so cabozantinib has strong theoretical potential as an effective targeted NSCLC therapy. A clinical trial comparing cabozantinib to erlotinib and a combination therapy of the two on patients with wild-type EGFR saw significant increases in progression free survival (PFS) when patients were treated with cabozantinib (4.3 months) or an erlotinib-cabozantinib combination (4.7 months) compared to erlotinib alone (1.8 months)<sup>36</sup>. However, it must be noted that this trial compared the drugs in patients with wild-type EGFR, whereas EGFR with activating mutations shows a significantly higher response rate to erlotinib than wild-type EGFR. However, it does illustrate that cabozantinib has potential as a treatment for NSCLC, especially considering the lack of patient stratification in the study. Another clinical trial treated patients with EGFR activating mutations who had previously undergone EGFR TKI therapy with a combination of erlotinib and cabozantinib in the hopes of overcoming acquired resistance. However, median progression free survival was comparatively low at 3.6 months, although interestingly T790M mutation status did not have a significant effect on PFS in patients where it was detected. Detection of

MET amplification in the overall population was unfortunately impossible, as only 10 out of 37 patients had tissue available for testing<sup>37</sup>.

It is clear that successful treatment with cabozantinib to overcome resistance in NSCLC requires further patient stratification. The detection of MET amplification to assess the effectiveness of the drug when amplification is present would be the next logical step. The testing of cabozantinib effectiveness after treatment with other EGFR TKIs such as gefitinib and afatinib to determine whether the inhibitor used in initial treatment affects the development of MET amplification as a resistance mechanism (and thus patient responses to cabozantinib) may also yield interesting results.

As a common element of both the MET and EGFR signalling pathway, a MEK inhibitor could also carry potential as a therapy to overcome EGFR inhibitor resistance. Trametinib is a MEK 1 and 2 inhibitor which is most commonly used in combination with BRAF inhibitors in metastatic melanoma with the V600E BRAF mutation, although this combination has also seen some use in NSCLC with the same mutation<sup>38</sup>.



**Figure 1.3 Simplified diagram of MET and EGFR pathway crosstalk.**

Preclinical studies have indeed shown that trametinib in combination with other drugs is able to overcome EGFR inhibitor-mediated resistance. In the first study, NSCLC cells were treated with WZ4002 (an irreversible third generation EGFR TKI) and trametinib and the results compared to cells treated with just WZ4002; the combination therapy delayed the onset of resistance when compared to WZ4002 monotherapy in an *in vitro* model and even resulted in complete remission in some *in vivo* mouse xenograft models. Unfortunately, however, in most cases resistance appeared once again, primarily attributed to a shift to PI3K signalling instead of the MAPK pathway<sup>39</sup>. In the second study, gefitinib and afatinib resistant NSCLC cells were treated with trametinib, taselisib (PI3K inhibitor) or a combination of both. The results demonstrated that the combination was significantly more effective than either drug on its own both *in vitro* and *in vivo*, probably as inhibition of both pathways make it more difficult for the cells to compensate for inhibition of one pathway by upregulating the other. Of further interest is the fact that the combination was effective against both T790M mutated cells and cells with MET amplification<sup>40</sup>. Whilst this study showed that trametinib as a monotherapy was not effective against gefitinib or afatinib resistant cells, it is not known whether erlotinib-resistant cells would continue this trend.

### 1.5.2. Metabolic changes arising in resistance

The drug responses of cancer cells are intrinsically coupled to their glucose metabolisms, and thus so is the generation of resistance. In the context of EGFR TKI resistant NSCLC cells specifically, the growth of cells resistant to erlotinib are more sensitive to glucose deprivation<sup>41</sup>, which is a phenomenon that could be exploited through drug therapy in an attempt to overcome resistance. Furthermore, upregulation of glycolysis and subsequent downregulation of oxidative phosphorylation (known as the Warburg effect) may guide cells into an increased state of anti-apoptosis due to decreases in electron transport chain activation in the mitochondria, which also regulates elements of the intrinsic apoptotic pathway<sup>42</sup>. Dichloroacetate (DCA) is a pyruvate dehydrogenase kinase (PDK) inhibitor whose mechanism of action results in decreased glycolysis, and has the potential to overcome this shift in cellular metabolism, especially if EGFR TKI resistance results in an additional shift towards a Warburg metabolism. While it has been previously demonstrated that DCA decreased lactate production and glucose consumption in NSCLC cells<sup>43</sup>, its potential in overcoming resistance to EGFR inhibitors has not yet been explored in depth. However, the fact that erlotinib-resistant tumours demonstrate increased lactate production and glucose consumption compared to untreated tumours *in vivo*<sup>44</sup> highlights that this is an area that warrants further exploration.

Interestingly, dichloroacetate is also able to increase the induction of apoptosis in NSCLC cells through the inhibition of autophagy<sup>45</sup>, a “survival-promoting pathway that captures, degrades, and recycles intracellular proteins and organelles in lysosomes”, allowing the cell to recycle its components and sustain itself metabolically in times of

decreased substrate availability as well as preventing the accumulation of toxic waste products<sup>46</sup>. Autophagy has been shown to increase in NSCLC cells treated with erlotinib and gefitinib (with an accompanied inhibition of the PI3K pathway)<sup>47</sup>, so DCA may have additional potential if it is successfully able to inhibit autophagy in EGFR TKI resistant cells.

## **1.6. Project aims and objectives**

While EGFR tyrosine kinase inhibitors are more effective treatments compared to classical chemotherapy in patients whose tumours harbour EGFR-activating mutations, the problem of acquired resistance remains. This project aims to characterise the generation and heterogeneity of resistance to erlotinib (first generation EGFR TKI), gefitinib (first generation EGFR TKI) and afatinib (second generation EGFR TKI) in an *in vitro* non-small cell lung cancer model composed of two distinct NSCLC adenocarcinoma cell lines both harbouring exon 19 deletions.

### Objectives:

1. Qualitatively examine differences in cell and monolayer morphology between the resistant cell lines and the parental cells to determine growth patterns.
2. Generate growth curves for the parental and resistant cells for comparison.
3. Screen resistant cell lines against a panel of anti-cancer drugs to test for cross-resistance and sensitivity when compared to parental cells.

## 2.0. Materials and Methods

### 2.1. Cell lines

HCC827 (HCC827 PTL) and HCC4006 (HCC4006 PTL) cell lines were used in the investigation into EGFR inhibitor resistance. Six EGFR TKI resistant sub-lines were also used: HCC827 adapted to 2 $\mu$ M erlotinib (HCC827 rErlo), HCC827 adapted to 2 $\mu$ M gefitinib (HCC827 rGefi), HCC827 adapted to 50nM afatinib (HCC827 rAfa), HCC4006 adapted to 1 $\mu$ M erlotinib (HCC4006 rErlo), HCC4006 adapted to 1 $\mu$ M gefitinib (HCC4006 rGefi) and HCC4006 adapted to 100nM Afatinib (HCC4006 rAfa). Resistant cell lines were obtained from the Resistant Cancer Cell Line (RCCL) collection at the University of Kent courtesy of Prof. Martin Michaelis.

(<https://research.kent.ac.uk/industrial-biotechnology-centre/the-resistant-cancer-cell-line-rccl-collection/><sup>48</sup>). Briefly, prior to the project commencing resistant cell lines were generated by dose-escalation with the respective drug until the maximum tolerance threshold was reached.

### 2.2. Cell culture

All cell lines were grown in separate T75 tissue culture flasks (Sarstedt) using 20ml Iscove's modified Dulbecco's medium (IMDM) (Gibco) supplemented with 10% v/v foetal bovine serum (FBS) (Sigma) and 1% v/v penicillin-streptomycin (Gibco). Cells were grown until they reached 70-80% confluency then split into new flasks at varying ratios. When passaging, cells were first washed with PBS, then dissociated from the flask using 0.25% trypsin-EDTA (Gibco). Fresh media was added every time cells were passaged. For drug-adapted cell lines, fresh drug was added to the media after each split. For HCC827 cells resistant to erlotinib and gefitinib (Selleckchem), the media



contained a final concentration of 2 $\mu$ M. For HCC827 cells resistant to afatinib, the media was made to a final concentration of 50nM afatinib (Selleckchem). For HCC4006 cells resistant to erlotinib and gefitinib, a final concentration of 1 $\mu$ M of each respective drug was used. For HCC4006 cells resistant to afatinib, the final concentration in the media was 100nM of afatinib.

### **2.3. xCELLigence growth assay**

At 70-80% confluency, cells were washed, trypsinised and resuspended in 10ml media to perform a cell count. Cells were then diluted to a seeding density of 5000 cells per well and seeded into 16 well RTCA plates; each cell line using 4 wells per plate for technical repeats. Cells were left to settle in the plates for 30 minutes, then inserted into the xCELLigence RTCA machine (ACEA Biosciences). The software was programmed to measure the cell index every 30 minutes for 144 hours to generate a growth curve. Three independent replicates were performed for each cell line.

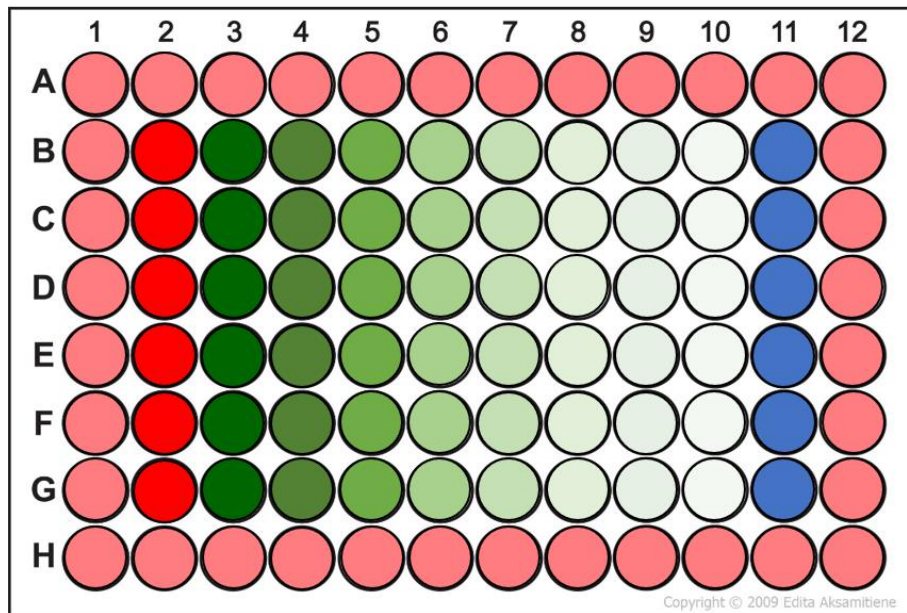
### **2.4. SRB assay**

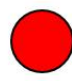

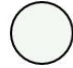


Drugs were made up in a 96 well drug block. Stock concentrations of each drug were diluted in media so that the concentration of the vehicle dimethyl sulfoxide (DMSO) did not exceed 0.1%, eliminating the need for a vehicle control. Starting concentrations were serially diluted to provide 8 different concentrations per drug. When cells were at 70-80% confluency in a T75 flask, they were washed, trypsinised and resuspended in 10ml fresh media. A cell count was taken, and cells were then diluted in media to a seeding density of 5,000 cells per well in a 96 well plate.

80 wells of a 96 well plate were used for each experiment. The remaining 16 were filled with 50 $\mu$ l media to prevent evaporation during the incubation period.

After seeding the 96 well plates with cells, the drugs were added to the seeded wells. The plates were left to incubate for 120 hours, then were fixed with 10% trichloroacetic acid (TCA) for 30 minutes. The plates were then rinsed with distilled water, after which they were then stained with 0.1% sulforhodamine B (SRB) for 30 minutes. The SRB was then washed out with 1% acetic acid, and the plates were left to dry overnight at 37°C. The plates were then solubilised with 10mM tris and left on the shaker at 300 rpm for 10 minutes. They were then read using a Victor X4 multilabel plate reader (PerkinElmer Life Sciences).

Absorbance of the treated cells was then calculated as a percentage of that of the untreated cells (subtracting the value of the empty control for both) to determine cell viability at each concentration of drug and subsequently generate a dose-response curve. Mean IC50 values (from technical repeats) for each replicate were calculated using GraphPad PRISM 6, which were then used to calculate the mean IC50 between biological replicates as well as the standard deviation. Three independent biological replicates were performed per drug and cell line.



-  Untreated cells
-  to  Cells treated with 8-point serial dilution
-  Empty control (100µl media)
-  50µl media

**Figure 2.1 96-well plate layout of SRB assay**  
 adapted from Edita Aksamitiene (2009)

### 3.0. Results

#### 3.1. Morphological and growth characterisation of parental and resistant cell lines

The non-small cell lung cancer cell lines HCC827 and HCC4006 were selected for this project as they contain activating mutations in the EGFR tyrosine kinase domain<sup>49,50</sup>.

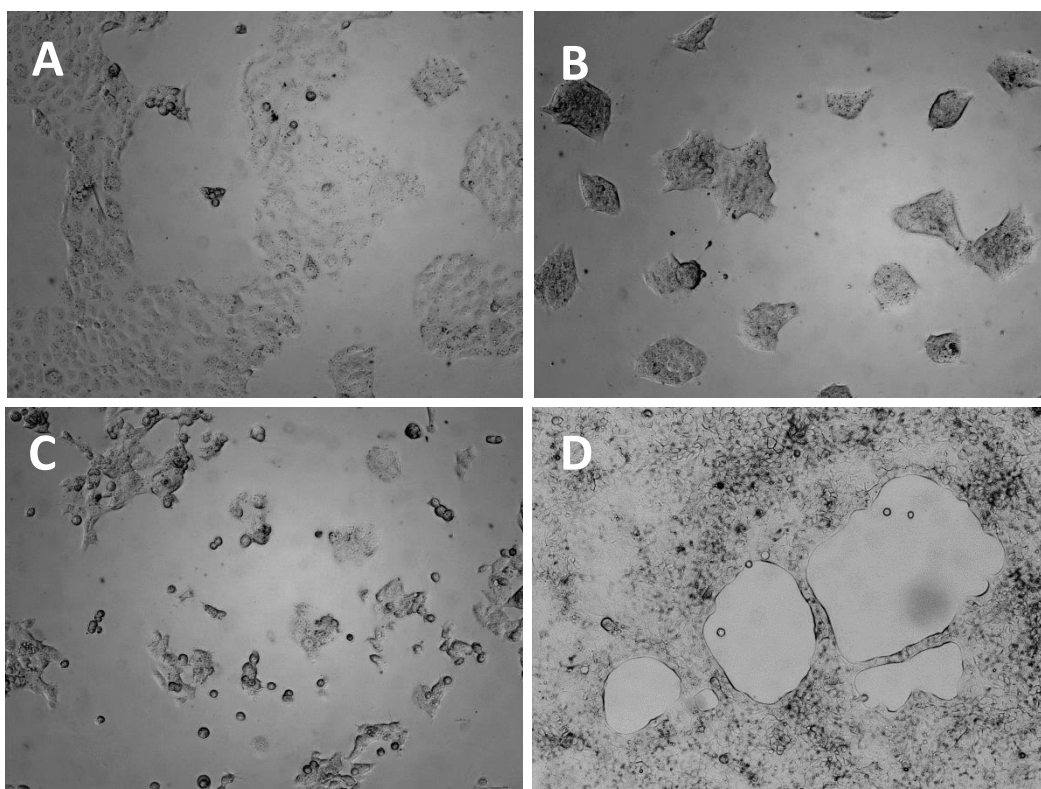
In order to characterise EGFR TKI resistance in these cell lines, three resistant sub-lines each of HCC827 and HCC4006 were acquired from the Resistant Cancer Cell Line collection (RCCL)<sup>48</sup>. The 3 sub-lines had previously been made resistant to Erlotinib (first generation EGFR TKI), Gefitinib (first generation EGFR TKI) and Afatinib (second generation EGFR TKI) respectively, through dose escalation. This results in 8 distinct cell lines, including the parental cell lines. The final concentration of drug that each sub-line is resistant to and was subsequently cultured in is outlined in table 3.2.

**Table 3.1 Non-small cell lung cancer cell lines used and associated EGFR status.** The amino acid deletions in both cell lines are caused by exon 19 deletions in the *EGFR* gene. Disease type and EGFR status for HCC827 and HCC4006 found at <https://www.atcc.org/products/all/CRL-2868.aspx> and <https://www.atcc.org/products/all/CRL-2871.aspx> respectively.

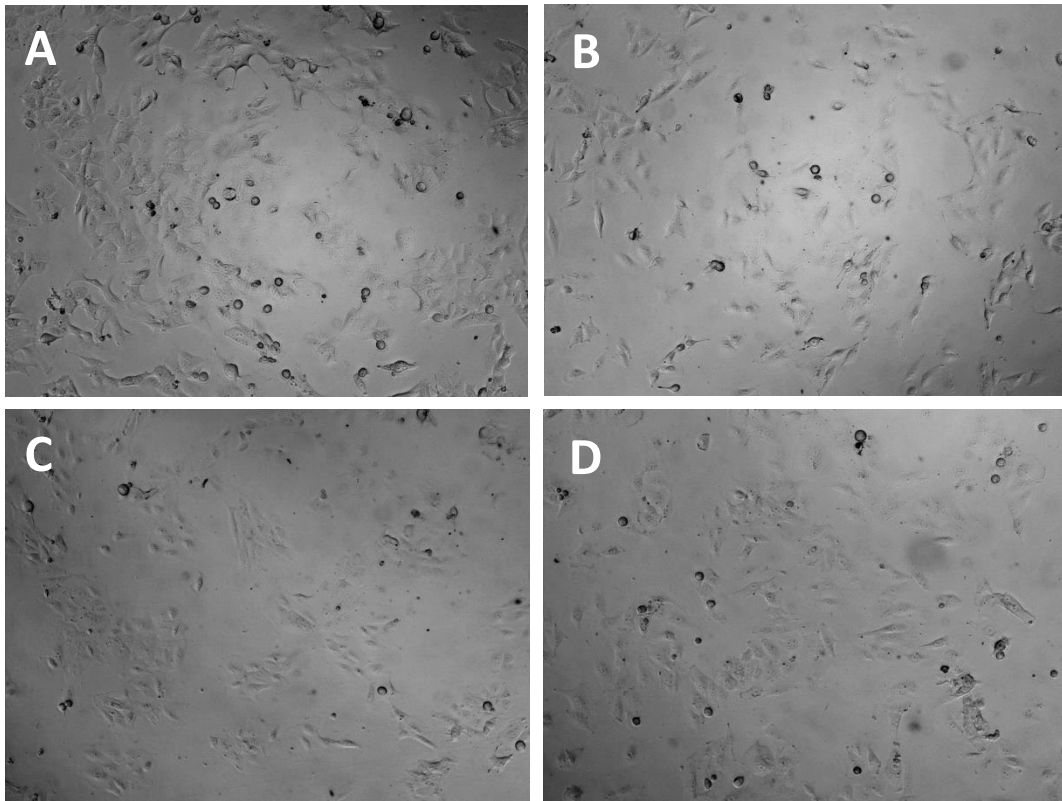
Cell line	Cell type	Disease type	EGFR status
HCC827	Epithelial	Lung adenocarcinoma	E746-A750 deletion
HCC4006	Epithelial	Lung adenocarcinoma (derived from metastatic site)	L747-E749 deletion, A750P substitution

**Table 3.2 Sub-line cell culture drug concentration**

<b>Cell Line</b>	<b>Final drug concentration</b>
HCC827 parental (HCC827 PTL)	No drug
HCC827 resistant to erlotinib (HCC827 rEro)	2 $\mu$ M
HCC827 resistant to gefitinib (HCC827 rGefi)	2 $\mu$ M
HCC827 resistant to afatinib (HCC827 rAfa)	50 nM
HCC4006 parental (HCC4006 PTL)	No drug
HCC4006 resistant to erlotinib (HCC4006 rEro)	1 $\mu$ M
HCC4006 resistant to gefitinib (HCC4006 rGefi)	1 $\mu$ M
HCC4006 resistant to afatinib (HCC4006 rAfa)	100 nM



**Figure 3.1 Phase contrast microscopy of HCC827 sub-lines in culture.** A: HCC827 parental cells. B: HCC827 cells resistant to Erlotinib. C: HCC827 cells resistant to Gefitinib D: HCC827 cells resistant to Afatinib. Images taken at 40X magnification on an Olympus CKX53 microscope.



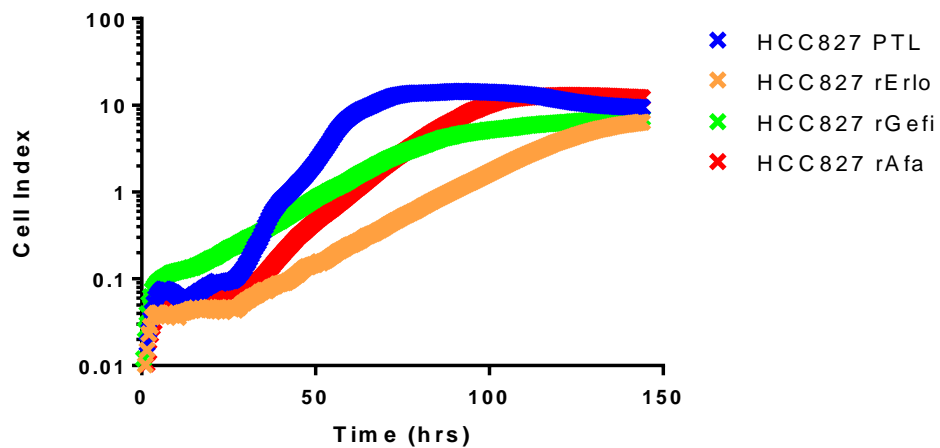
**Figure 3.2 Phase contrast microscopy of HCC4006 sub-lines in culture.** A: HCC4006 parental cells. B: HCC4006 cells resistant to Erlotinib. C: HCC4006 cells resistant to Gefitinib D: HCC4006 cells resistant to Afatinib. Images taken at 40X magnification on an Olympus CKX53 microscope.

Phase contrast microscopy images were taken of each of the 8 cell lines to qualitatively compare physical cell and growth morphology. As seen in figure 3.1, whilst the HCC827 PTL cells appear flatter and more spread out and tend to grow in a flat monolayer, HCC827 rErlo cells grew more in clusters, with layers of cells growing on top of each other in distinct colonies. HCC827 rGefi cells appear to reflect a nature in between HCC827 PTL and HCC827 rErlo, with a more clustered structure than the former but in a flatter manner than the latter. HCC827 rAfa also have a distinct morphology, appearing to be smaller in size than the parental cells. However in contrast to HCC827 rErlo and HCC827 rGefi, they tend to grow more in a monolayer.

The qualitative difference in morphology between parental and resistant cells for the HCC4006 sub-lines appears less stark; as seen in figure 3.2, all 4 HCC4006 sub-lines

tend to grow in a flat monolayer, with no apparent clustering present. HCC4006 PTL, HCC4006 rErlo and HCC4006 rGefi cells also appear to be of similar sizes, while HCC4006 rAfa appear slightly larger than the others.

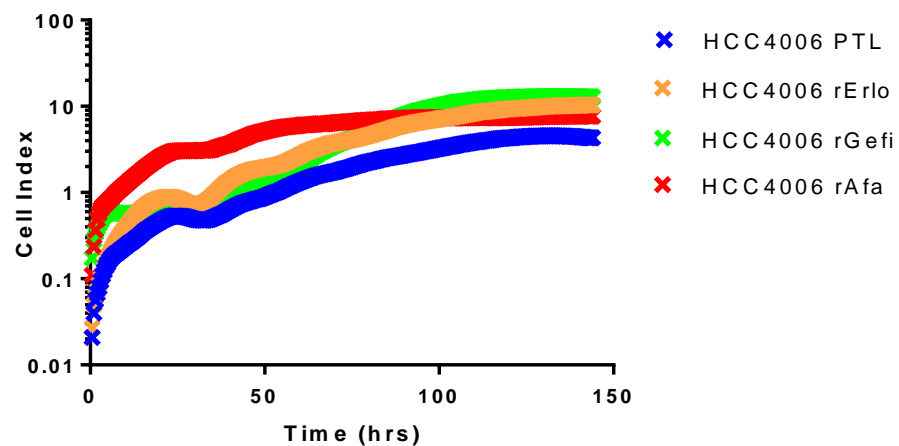
### A HCC827 Resistant Cell Line Growth Curve



### B

	HCC827 PTL	HCC827 rErlo	HCC827 rGefi	HCC827 rAfa
Doubling time (hrs)	7.22	14.22	14.40	9.55

### C HCC4006 Resistant Cell Line Growth Curve



### D

	HCC4006 PTL	HCC4006 rErlo	HCC4006 rGefi	HCC4006 rAfa
Doubling time (hrs)	21.65	23.25	15.44	26.32

**Figure 3.3 Growth curves and doubling times of HCC827 and HCC4006 sub-lines.** A: HCC827 sub-line growth curves. B: HCC827 sub-line doubling times. C: HCC4006 sub-line growth curves. D: HCC4006 sub-line doubling times. Growth curves were generated by xCELLigence real-time cell analysis (ACEA). Plates were seeded at 5000 cells per well in a 16-well format, with 4 technical repeats per cell line and 4 cell lines per plate. Cell Index was measured every 30 minutes over a period of 6 days (144 hours). All data are representative of 3 independent experiments.



Growth curves were also generated through xCELLigence real-time cell analysis (RTCA) for each sub-line as part of the characterisation process, allowing for the drugs that slow the growth of cells the most to be identified, which could have important clinical implications for tumour growth. Doubling times for each sub-line were calculated using the following formula, with concentration values taken when the cells were in the log growth phase:

$$\text{Doubling time} = \frac{\text{Duration} * \log(2)}{\log(\text{Final Concentration}) - \log(\text{Initial Concentration})}$$

For the HCC827 sub-lines, HCC827 PTL and HCC827 rAfa are the cell lines that demonstrated the fastest doubling time, while HCC827 rErlo and HCC827 rGefi grew somewhat slower; this appears to demonstrate that first generation EGFR inhibitors are more likely to impede cell growth once resistance has developed when compared to afatinib (a second generation inhibitor), which appears to result in a faster rate of cell division. The slight drops seen in the growth curve after the initial plateau (most apparent in HCC827 PTL but also present in HCC827 rAfa) are likely due to overcrowding in the wells, leading to cells undergoing apoptosis and detaching from the bottom of the well, decreasing the Cell Index.

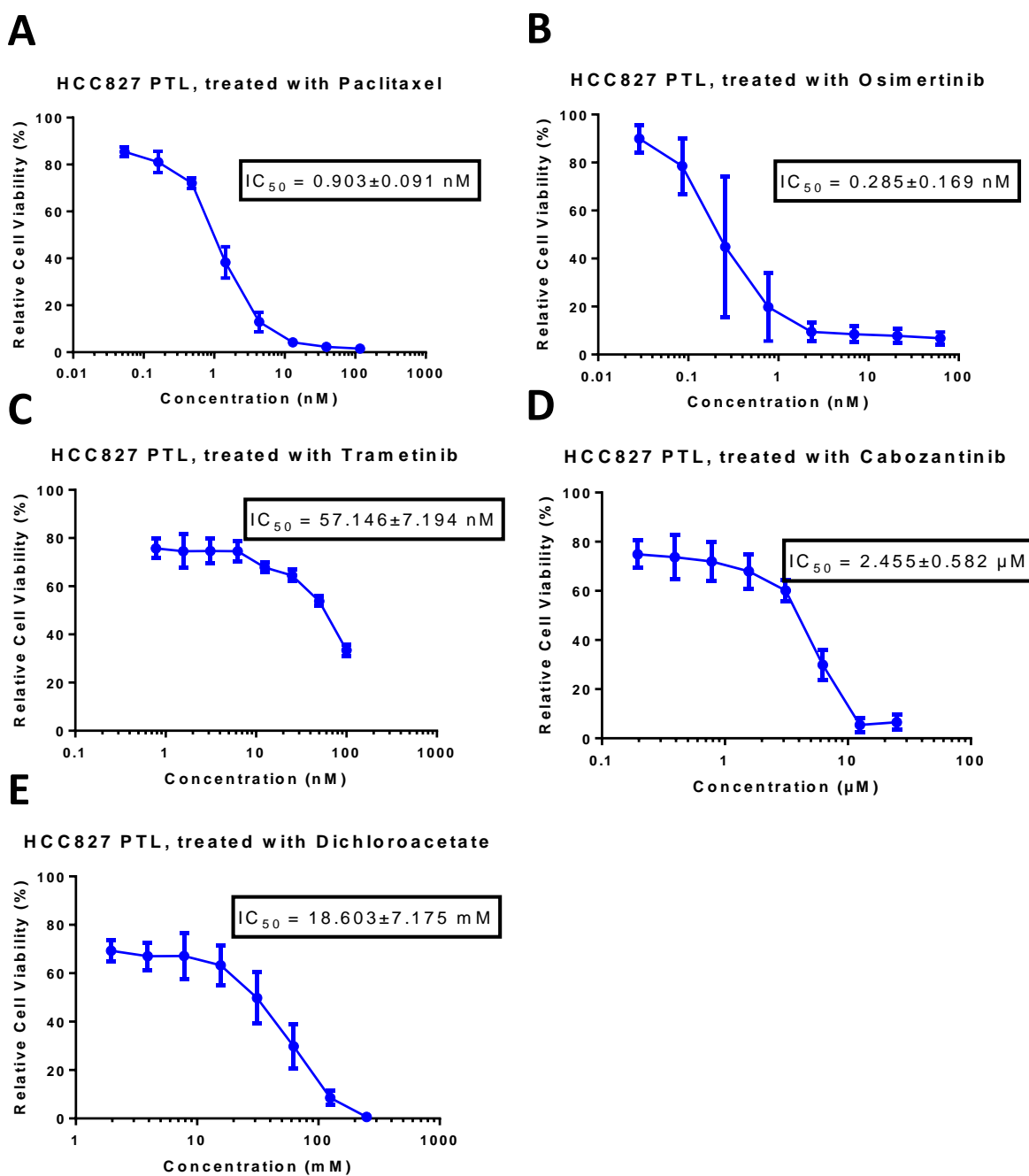
However, it must be taken into account that the xCELLigence system generates growth curves based on cells impeding the electron flow between two electrodes, where the more surface area is covered by the cells the higher the impedance is, and that HCC827 rErlo and HCC827 rGefi tend to grow in clusters on top of each other rather than spreading over a wider surface area (which is characteristic of HCC827 PTL and HCC827 rAfa), and this may affect the results of the assay. Future work should thus

include comparison with an alternative method of generating cell growth curves, for example a cell density seeding assay.

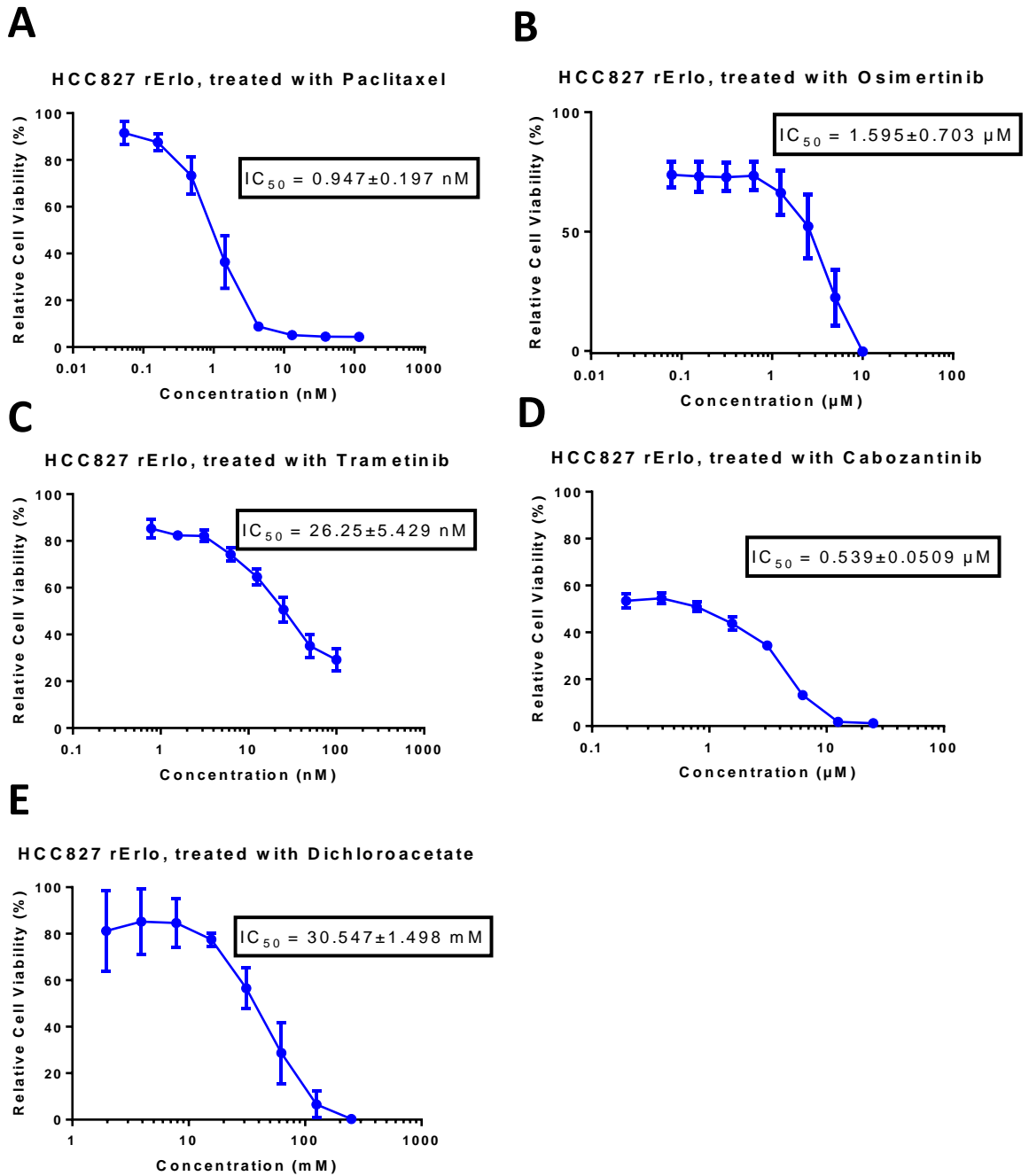
By comparison, the parental cell line for the HCC4006 sub-lines is not the fastest-growing cell lines, growing slower than HCC4006 rGefi. It also has the lowest final Cell Index of the sub-lines, meaning that it has the fewest cells in the wells at the end of the 6 day period. Meanwhile, HCC4006 rAfa shows the highest initial growth rate (although it has the slowest doubling time at 26.32 hours) and HCC4006 rGefi has the lowest doubling time by far at 15.44 hours (~6 hours lower than the next-fastest growing sub-line, HCC4006 PTL) as well as the highest final Cell Index, and is thus overall the fastest-growing HCC4006 sub-line. HCC4006 rErlo meanwhile sits somewhere between HCC4006 rGefi and HCC4006 PTL with a doubling time of 22.92 hours. Interestingly, both HCC4006 rGefi and HCC4006 rErlo sub-lines grow faster than the parental cell line whereas, unlike in HCC827, afatinib appears to slow growth as demonstrated by HCC4006 rAfa. This serves to highlight the underlying heterogeneity found in the context of acquired drug resistance; despite hailing from the same original tissue type and harbouring similar EGFR-activating mutations, their response to the drugs they become resistant to is very different.

As the growth curves have been generated while the cells are in culture conditions containing concentrations of drug that they are resistant to (with the obvious exception of the parental cell lines), it would be interesting to compare them to growth curves of resistant cells grown without drug present to compare whether there is a significant difference. Additionally, it would be interesting to compare the growth rates of the cell lines in the context of a typical EGFR inhibitor patient dosing regimen to better simulate the clinical usage pattern of the drugs.

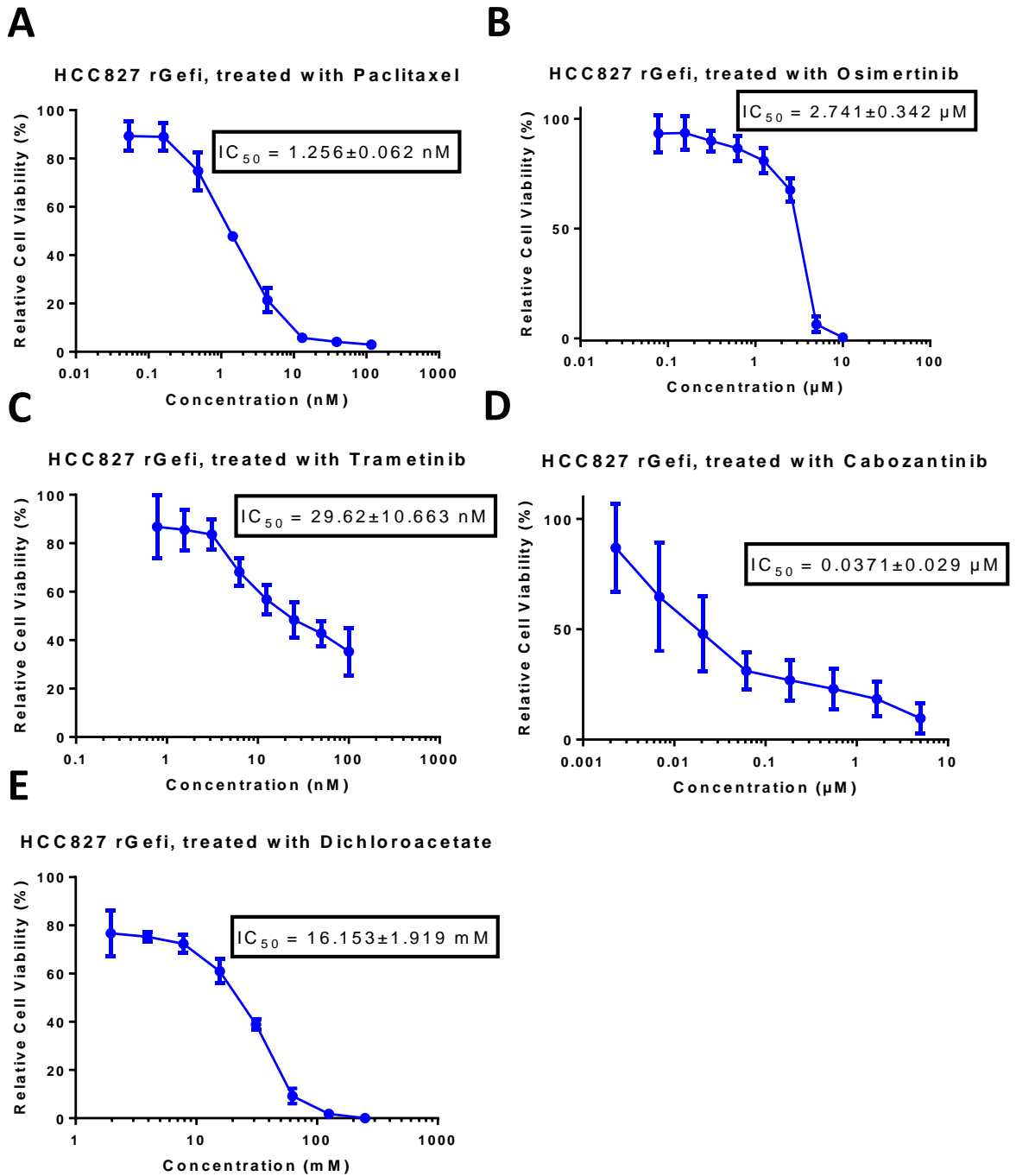
### 3.2. IC50 characterisation of parental and resistant cell lines



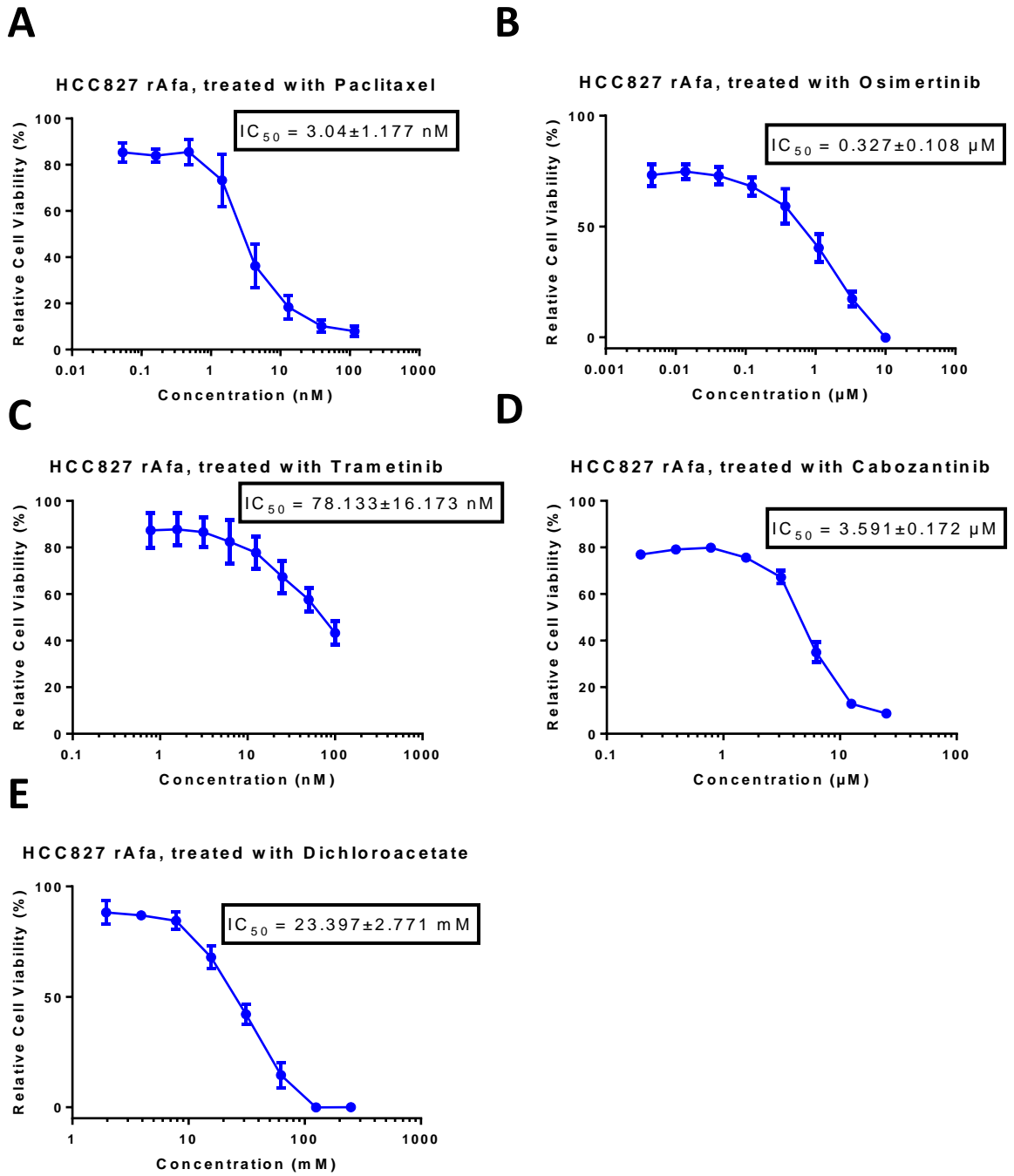
**Figure 3.4** Dose-response curves of HCC827 PTL cells treated with anti-cancer drug panel. A: HCC827 PTL treated with Paclitaxel. B: HCC827 PTL treated with Osimertinib. C: HCC827 PTL treated with Trametinib. D: HCC827 PTL treated with Cabozantinib. E: HCC827 PTL treated with dichloroacetate. Data were collected using SRB assays and  $IC_{50}$  was calculated with GraphPad Prism 6. All data (including  $IC_{50}$  values) are the mean of 3 independent experiments, with error bars representing  $\pm$  standard deviation.



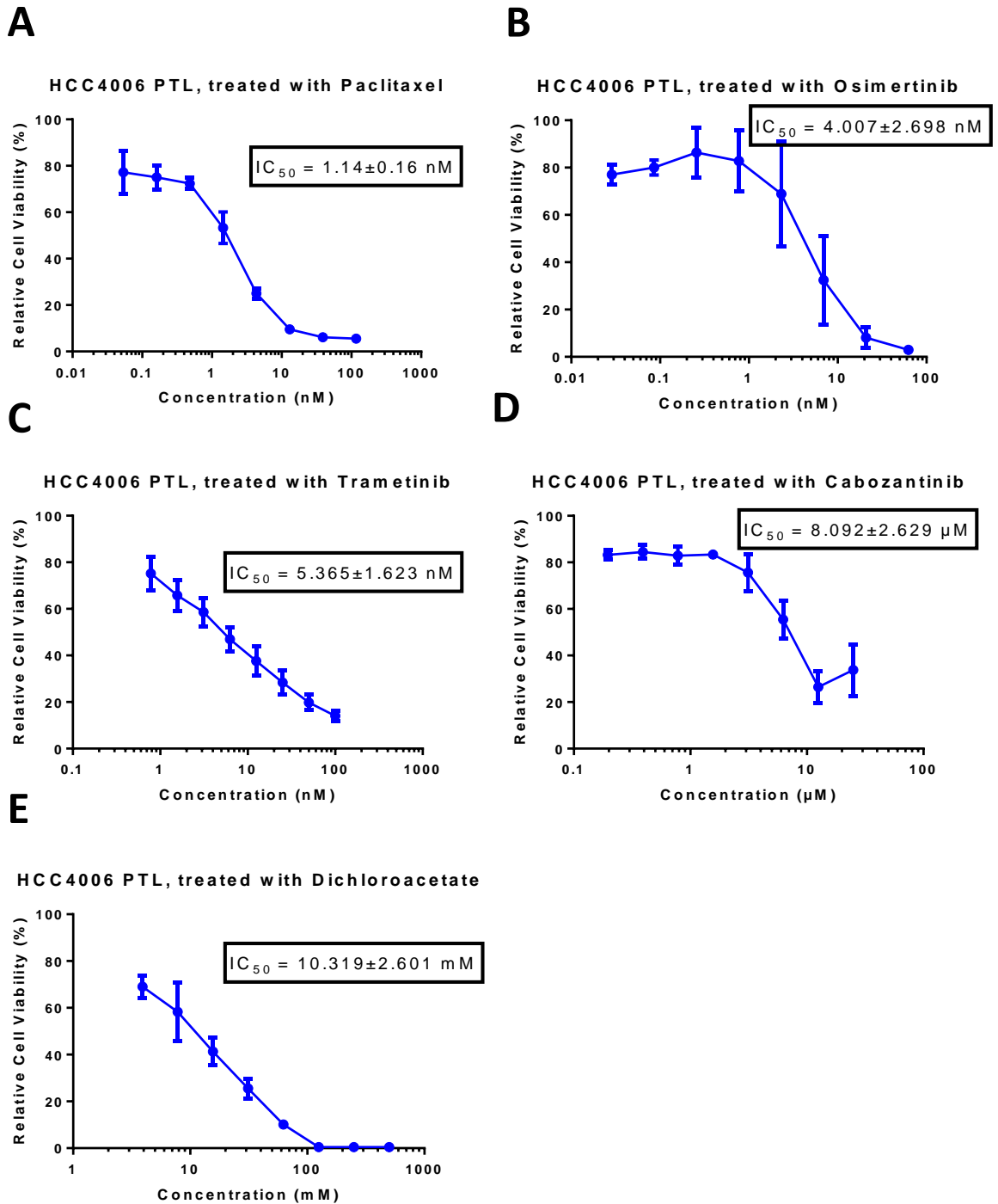
**Figure 3.5 Dose-response curves of HCC827 rErlo cells treated with anti-cancer drug panel.** A: HCC827 rErlo treated with paclitaxel. B: HCC827 rErlo treated with osimertinib. C: HCC827 rErlo treated with trametinib. D: HCC827 rErlo treated with cabozantinib. E: HCC827 rErlo treated with dichloroacetate. Data were collected using SRB assays and IC<sub>50</sub> was calculated with GraphPad Prism 6. All data (including IC<sub>50</sub> values) are the mean of 3 independent experiments, with error bars representing  $\pm$  standard deviation.



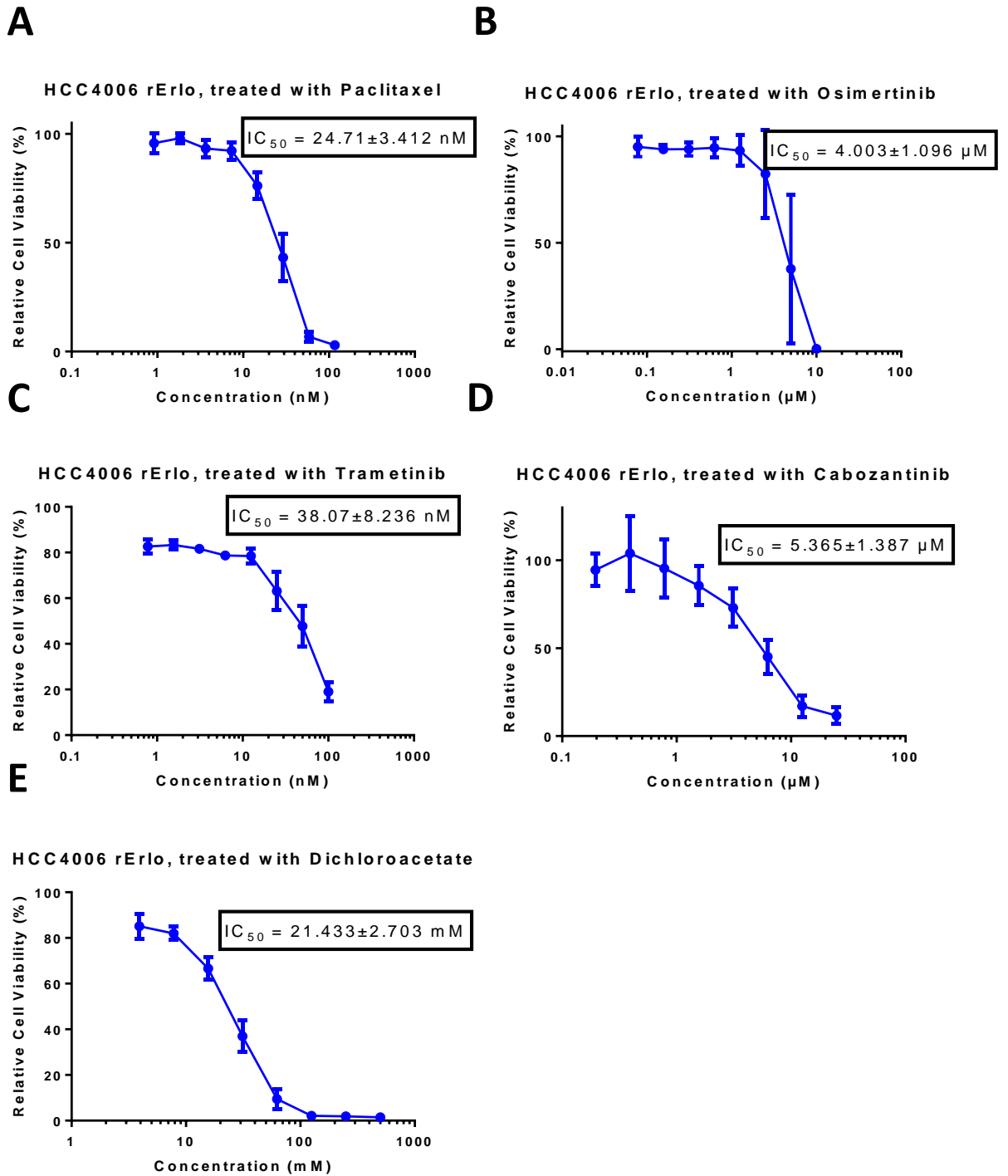
**Figure 3.6 Dose-response curves of HCC827 rGefi cells treated with anti-cancer drug panel.** A: HCC827 rGefi treated with paclitaxel. B: HCC827 rGefi treated with osimertinib. C: HCC827 rGefi treated with trametinib. D: HCC827 rGefi treated with cabozantinib. E: HCC827 rGefi treated with dichloroacetate. Data were collected using SRB assays and  $IC_{50}$  was calculated with GraphPad Prism 6. Data (including  $IC_{50}$  values) for paclitaxel, osimertinib, trametinib and dichloroacetate treated cells are the mean of 3 independent experiments. Data for cabozantinib treated cells are the mean of 2 independent experiments. Error bars represent  $\pm$  standard deviation.



**Figure 3.7 Dose-response curves of HCC827 rAfa cells treated with anti-cancer drug panel.** A: HCC827 rAfa treated with paclitaxel. B: HCC827 rAfa treated with osimertinib. C: HCC827 rAfa treated with trametinib. D: HCC827 rAfa treated with cabozantinib. E: HCC827 rAfa treated with dichloroacetate. Data were collected using SRB assays and  $IC_{50}$  was calculated with GraphPad Prism 6. All data (including  $IC_{50}$  values) are the mean of 3 independent experiments, with error bars representing  $\pm$  standard deviation.

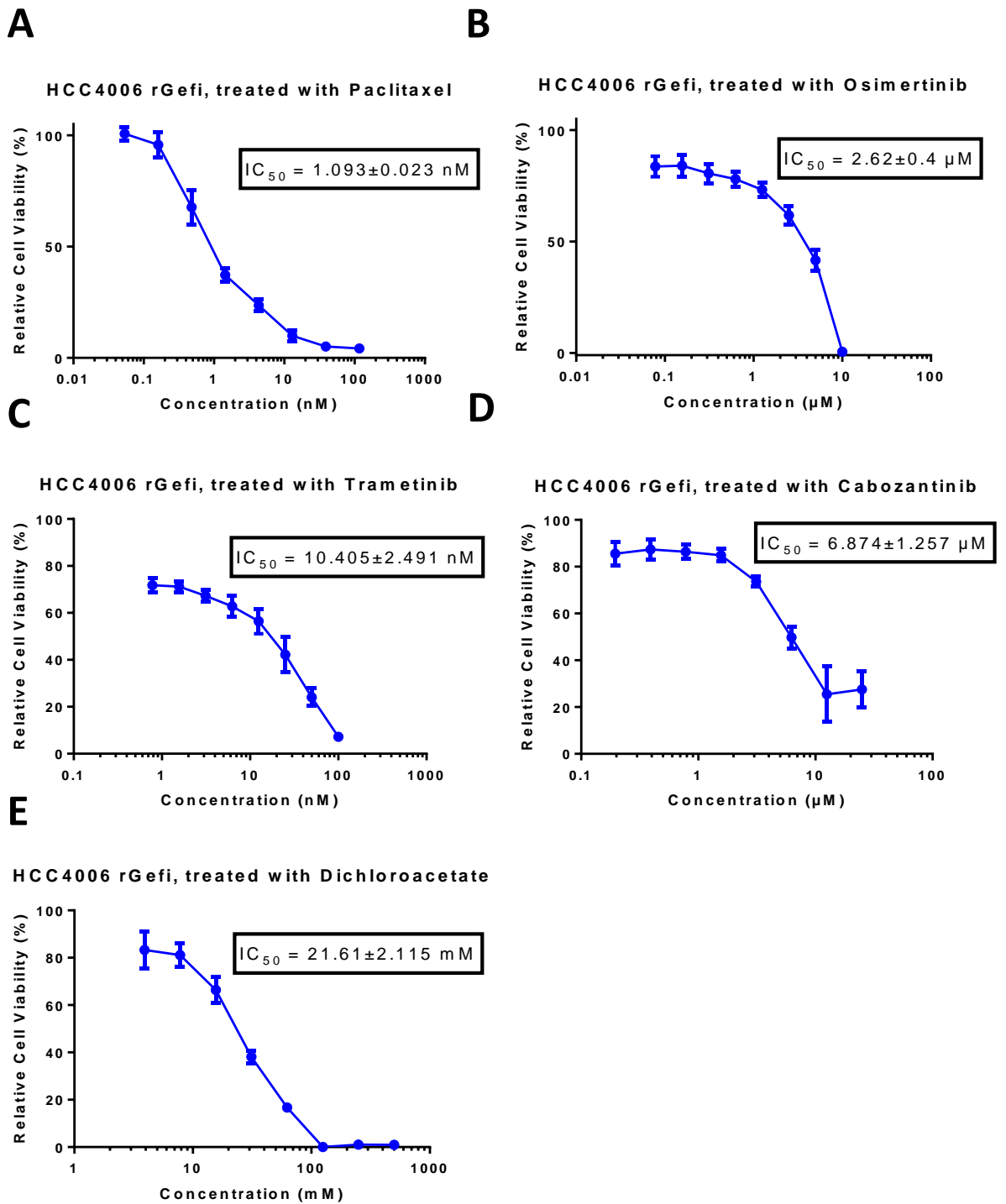


**Figure 3.8 Dose-response curves of HCC4006 PTL cells treated with anti-cancer drug panel.** A: HCC4006 PTL treated with Paclitaxel. B: HCC4006 PTL treated with Osimertinib. C: HCC4006 PTL treated with Trametinib. D: HCC4006 PTL treated with Cabozantinib. E: HCC4006 PTL treated with Dichloroacetate. Data were collected using SRB assays and  $IC_{50}$  was calculated with GraphPad Prism 6. All data (including  $IC_{50}$  values) are the mean of 3 independent experiments, with error bars representing  $\pm$  standard deviation.

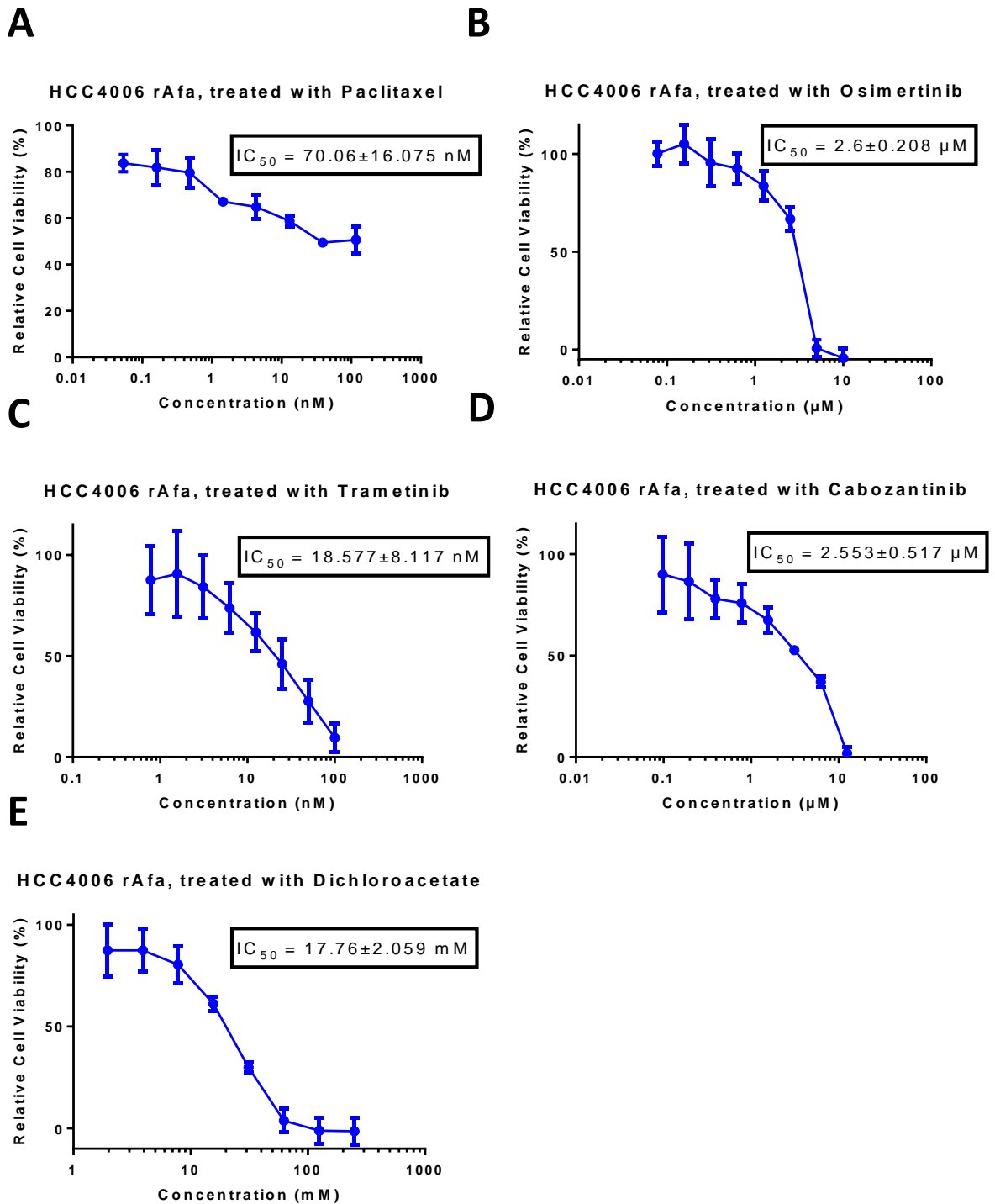


**Figure 3.9 Dose-response curves of HCC4006 rErlo cells treated with anti-cancer drug panel.** A: HCC4006 rErlo treated with Paclitaxel. B: HCC4006 rErlo treated with Osimertinib. C: HCC4006 rErlo treated with Trametinib. D: HCC4006 rErlo treated with Cabozantinib. E: HCC4006 rErlo treated with Dichloroacetate. Data were collected using SRB assays, and  $IC_{50}$  was calculated with GraphPad Prism 6. All data (including  $IC_{50}$  values) are the mean of 3 independent experiments, with error bars representing  $\pm$  standard deviation.





**Figure 3.10 Dose-response curves of HCC4006 rGefi cells treated with anti-cancer drug panel.** A: HCC4006 rGefi treated with Paclitaxel. B: HCC4006 rGefi treated with Osimertinib. C: HCC4006 rGefi treated with Trametinib. D: HCC4006 rGefi treated with Cabozantinib. E: HCC4006 rGefi treated with Dichloroacetate. Data were collected using SRB assays and  $IC_{50}$  was calculated with GraphPad Prism 6. All data (including  $IC_{50}$  values) are the mean of 3 independent experiments, with error bars representing  $\pm$  standard deviation.



**Figure 3.11 Dose-response curves of HCC4006 rAfa cells treated with anti-cancer drug panel.** A: HCC4006 rAfa treated with Paclitaxel. B: HCC4006 rAfa treated with Osimertinib. C: HCC4006 rAfa treated with Trametinib. D: HCC4006 rAfa treated with Cabozantinib. E: HCC4006 rAfa treated with Dichloroacetate. Data were collected using SRB assays and  $IC_{50}$  was calculated with GraphPad Prism 6. All data (including  $IC_{50}$  values) are the mean of 3 independent experiments, with error bars representing  $\pm$  standard deviation.

Continuing with the characterisation process, dose-response curves were generated for each HCC827 and HCC4006 sub-line for a panel of 5 anti-cancer drugs. The drug panel includes paclitaxel, osimertinib, trametinib, cabozantinib and dichloroacetate. Their mechanisms of action are summarised in table 3.3.

**Table 3.3 Anti-cancer drugs included in the screening panel and their respective mechanisms of action.**

<b>Drug</b>	<b>Mechanism of action</b>
Paclitaxel	Microtubule destabilisation inhibitor
Osimertinib	Third generation EGFR tyrosine kinase inhibitor
Trametinib	MEK inhibitor
Cabozantinib	MET inhibitor (also inhibits other RTKs with lower affinity)
Dichloroacetate	Pyruvate dehydrogenase kinase inhibitor

The IC50 for each drug/sub-line combination was then calculated to determine whether any sensitivity or cross-resistance is present in the resistant cell lines. IC50s were compared across the sub-lines for each drug (figure 3.12, figure 3.13) and the resistance factor for each resistant sub line (fold-resistance compared to the parental cell line) was calculated to allow for an effective comparison of the resistant sub-lines to the parental cells.

$$Resistance\ factor\ (RF) = \frac{resistant\ IC50}{parental\ IC50}$$

For the different HCC827 sub-lines that were treated with paclitaxel, it is clear that there is resistance to paclitaxel in HCC827 rAfa compared to the parental cells (table 3.4, figure 3.12 A), with a 3.38x higher IC50. Erlotinib and gefitinib, by contrast, show no significant differences, with resistance factors of 1.05 and 1.39 respectively compared the parental cell line. The HCC4006 drug-adapted sub-lines also showed

significant resistance to paclitaxel in HCC4006 rAfa, as well as a non-significant trend towards resistance in HCC4006 rErlo; interestingly, this is to a much greater extent than any of the HCC827 sub-lines, with resistance factors of 61.46 and 21.68 respectively. However, HCC4006 rGefi shows no significant resistance when compared to the parental cells, with a resistance factor of 0.96 (table 3.5, figure 3.13 A).

Interestingly, significant resistance is seen in both the EGFR TKI adapted HCC827 and HCC4006 cell lines compared to the parentals when treated with osimertinib (table 3.4, figure 3.12 B), a third-generation EGFR TKI that's designed specifically to overcome T790M resistance mutations, therefore suggesting that their resistance is due to an alternative mechanism. Amongst the HCC827 sub-lines, cells adapted to gefitinib had the highest rate of resistance with a fold-resistance of 9618, then the erlotinib resistant sub-line with an RF of 5600. Finally, the afatinib resistant cells which have an IC50 1147x higher than the parental cells, although this was not found to be statistically significant. Cross-resistance to osimertinib is somewhat less pronounced in the HCC4006 drug-adapted sub-lines, although comparatively it is still very high. This time, statistically significant differences were found across all sub-lines, with erlotinib attaining the highest resistance factor at 999, gefitinib having the second highest at 653, and finally afatinib with a resistance factor of 553.

When treated with the MEK inhibitor trametinib, the two HCC827 sublines resistant to first generation EGFR TKIs (erlotinib and gefitinib) actually had lower IC50s than the parental cell line, with a resistance factor of 0.46 and 0.52 respectively (although only erlotinib was found to be significant), and thus indicate increased sensitivity to the drug. However, the afatinib resistant cells have a higher IC50 value than the parental cell line and are thus resistant, although only by a comparatively low and statistically

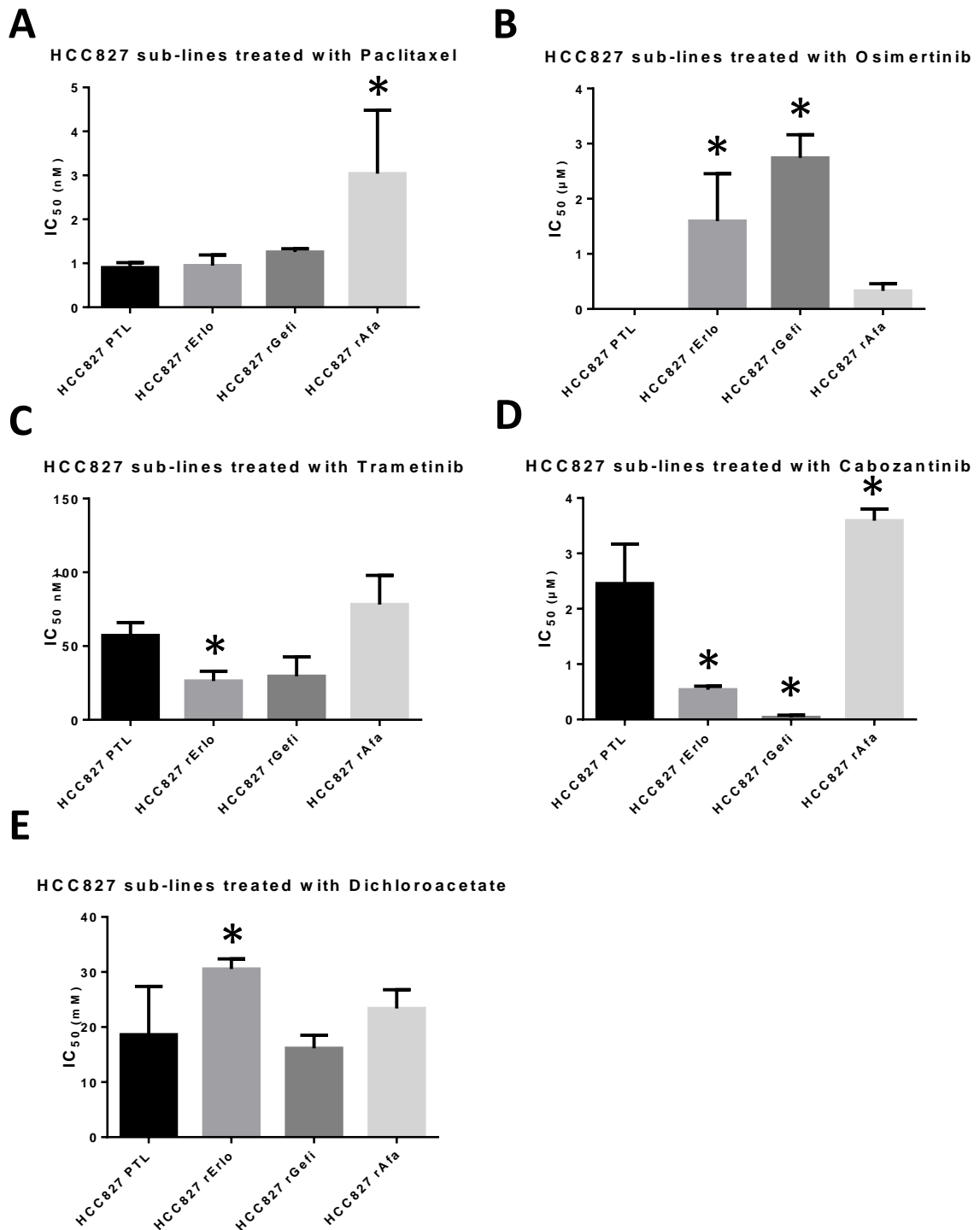
insignificant 1.37x (table 3.4, figure 3.12 C). Unlike the resistant HCC827 cell lines however, the resistant HCC4006 sub-lines all demonstrate an increased IC50 to trametinib when compared to the parental cells (table 3.5, figure 3.13 C), although once again only erlotinib reaches statistical significance; erlotinib shows the highest fold-resistance with an RF of 7.09, compared to nearly half that for afatinib at 3.56 and 1.94 for gefitinib. Also of note, the parental HCC4006 cell line has over a 10X lower IC50 for trametinib compared to the HCC827 parental cells (5.37 nM vs 57.15 nM), suggesting that HCC4006 PTL cells rely more on MAPK pathway activation than HCC827. Interestingly however, no change in sensitivity to trametinib is displayed by any HCC4006 resistant sub-lines, suggesting a decrease in MAPK pathway activation when treated with EGFR inhibitors (table 3.5, figure 3.13 C).

However, there is further sensitivity in erlotinib and gefitinib adapted HCC827 cells when treated with MET (among other receptor tyrosine kinases) inhibitor cabozantinib (table 3.4, figure 3.12 D); cells resistant to gefitinib showed the most sensitivity, with an IC50 that is just 1.5% that of the parental cells, or an RF of 0.015. Erlotinib adapted cells were also more sensitive than the parentals, although not to the same extent; with a resistance factor of 0.22, they are just over 4x more sensitive than the parental cells. However, as with trametinib, afatinib adapted cells again display a higher IC50 than the parental cells, around 1.46x (RF=1.46), indicating resistance. One of the EGFR TKI adapted HCC4006 sub-lines also display sensitivity to cabozantinib, with a resistance factor of 0.32 for the afatinib resistant cell line. The erlotinib and gefitinib resistant HCC4006 sub-lines also shows slight sensitivity with RFs of 0.55 and 0.85 respectively, but this is not statistically significant (table 3.5, figure 3.13 D).

Treating with dichloroacetate reveals no significant changes compared to the parental cells (HCC827 rGefi and rAfa sub-lines) or further resistance (HCC827 rErlo, all HCC4006 sub-lines). For the HCC827 cell lines, erlotinib-resistant cells have the highest IC50, resulting in a significant resistance factor of 1.64. HCC827 rAfa again demonstrates a trend towards resistance, with a resistance factor of 1.26 while gefitinib-adapted cells have a lower IC50 than the parental cells with an RF of 0.87 (although neither of these is statistically significant) (table 3.4, figure 3.12 E). The EGFR TKI resistant HCC4006 sub-lines also demonstrate cross-resistance when treated with DCA, with gefitinib and erlotinib having almost equal fold-resistance (2.09 and 2.07 times, respectively), with afatinib showing a slightly lower resistance factor of 1.79. All drug-adapted HCC4006 sub-lines thus demonstrate statistically significant resistance compared to the parental cells (table 3.5, figure 3.13 E).

**Table 3.4 IC50 comparison of HCC827 sub-lines treated with anti-cancer drug panel.**

<b>Drug</b>	<b>IC50 ±SD</b>			
	<b>HCC827 PTL</b>	<b>HCC827 rErlo</b>	<b>HCC827 rGefi</b>	<b>HCC827 rAfa</b>
Paclitaxel (nM)	0.903 ±0.091	0.947 ±0.196	1.256 ±0.062	3.04 ±1.177
Osimertinib (µM)	0.000285 ±0.000169	1.596 ±0.703	2.741 ±0.342	0.327 ±0.108
Trametinib (nM)	57.147 ±7.193	26.25 ±5.429	29.62 ±10.663	78.133 ±16.173
Cabozantinib (µM)	2.455 ±0.582	0.539 ±0.0509	0.037 ±0.029	3.59 ±0.172
Dichloroacetate (mM)	18.60 ±7.175	30.55 ±1.498	16.15 ±1.918	23.40 ±2.771



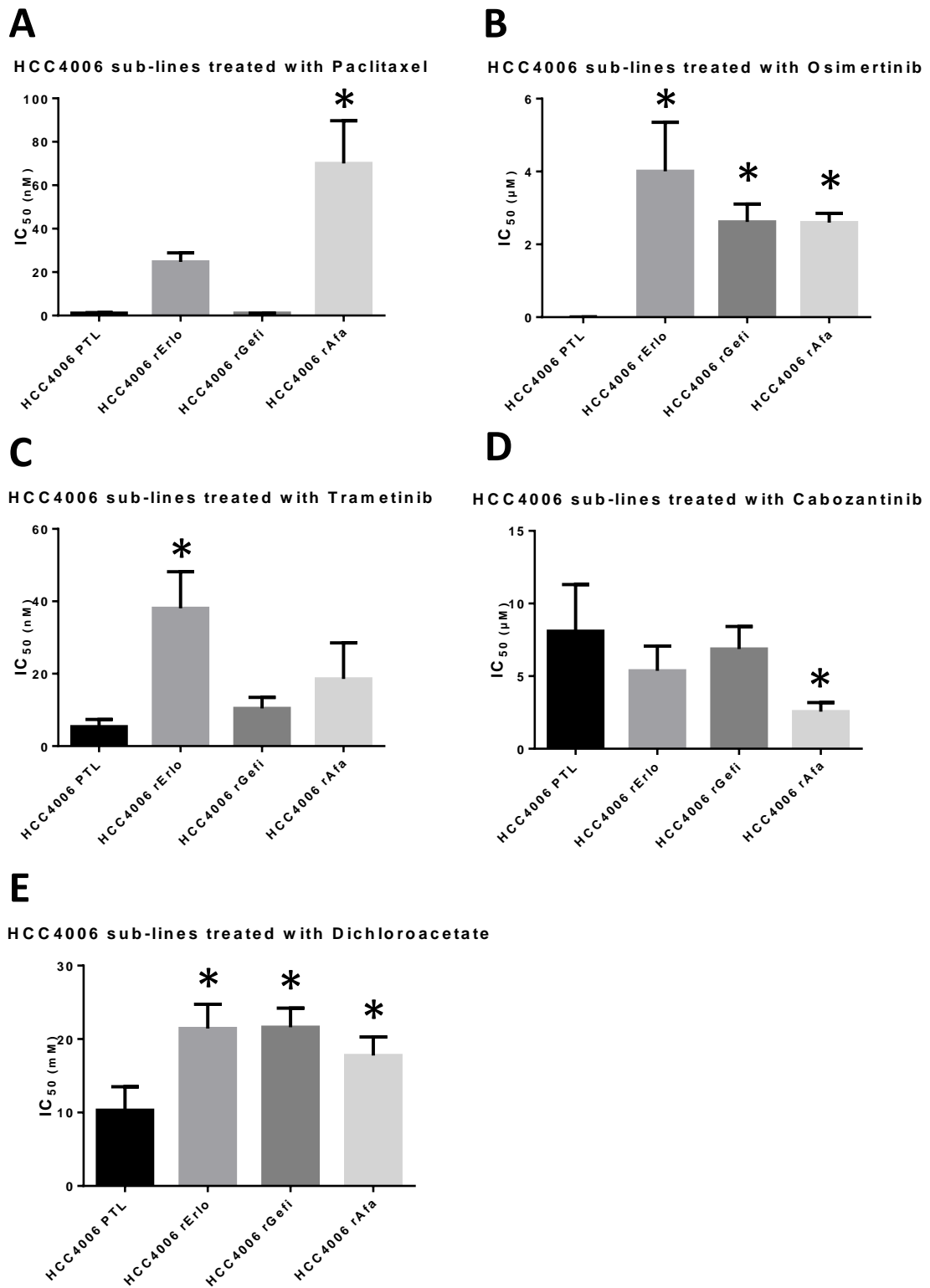
**Figure 3.12 IC<sub>50</sub> comparison of HCC827 sub-lines treated with anti-cancer drug panel.**

A: HCC827 sub-lines treated with Paclitaxel. B: HCC827 sub-lines treated with Osimertinib. C: HCC827 sub-lines treated with Trametinib. D: HCC827 sub-lines treated with Cabozantinib. E: HCC827 sub-lines treated with Dichloroacetate. Data were collected using SRB assays and IC<sub>50</sub> was calculated with GraphPad Prism 6. All data are the mean of 3 independent experiments except HCC827 rGefitinib treated with Cabozantinib, which is the mean of 2 independent experiments. Error bars represent standard deviation, \* =  $p < 0.05$ , one-way ANOVA with Dunnett's correction.



**Table 3.5 IC50 comparison of HCC4006 sub-lines treated with anti-cancer drug panel.**

<b>Drug</b>	<b>IC50 ±SD</b>			
	<b>HCC4006 PTL</b>	<b>HCC4006 rErlo</b>	<b>HCC4006 rGefi</b>	<b>HCC4006 rAfa</b>
Paclitaxel (nM)	1.139 ±0.159	24.71 ±3.412	1.093 ±0.023	70.06 ±16.075
Osimertinib (µM)	0.004007 ±0.00269	4.003 ±1.096	2.62 ±0.4	2.60 ±0.208
Trametinib (nM)	5.365 ±1.623	38.07 ±8.236	10.405 ±2.491	18.577 ±8.117
Cabozantinib (µM)	8.092 ±2.629	5.365 ±1.387	6.874 ±1.257	2.553 ±0.517
Dichloroacetate (mM)	10.319 ±2.601	21.433 ±2.703	21.61 ±2.115	17.76 ±2.059



**Figure 3.13 IC<sub>50</sub> comparison of HCC4006 sub-lines treated with anti-cancer drug panel.** A: HCC4006 sub-lines treated with Paclitaxel. B: HCC4006 sub-lines treated with Osimertinib. C: HCC4006 sub-lines treated with Trametinib. D: HCC4006 sub-lines treated with Cabozantinib. E: HCC4006 sub-lines treated with Dichloroacetate. Data were collected using SRB assays and IC<sub>50</sub> was calculated with GraphPad Prism 6. All data are the mean of 3 independent experiments. Error bars represent standard deviation, \*= p < 0.05, one-way ANOVA with Dunnett's correction.

## **4.0. Discussion**

The aim of this project was to characterise the EGFR-mutant non-small cell lung cancer cell lines HCC827 and HCC4006 and their sublines adapted to erlotinib, gefitinib or afatinib for their morphology, growth behaviour, and resistance to a panel of selected drugs.

### **4.1. Resistance affects cell growth and morphology**

The xCELLigence RTCA assay demonstrates that the sub lines' growth curves change in a drug and cell line-dependent manner. In the HCC827 sub lines, the parental cells retained the highest rate of growth, followed by HCC827 rAfa. HCC827 rGefi and HCC827 rErlo, which are both resistant to first-generation EGFR TKIs with very similar chemical structures, are shown to grow significantly slower. This is very interesting as this means there could be useful clinical implications associated with the decreased cell division rate; meaning that in some cases of NSCLC, even once the tumour has stopped responding directly to the drug, the treatment could still be slowing down the growth rate. However, it is important to bear in mind the morphological changes wrought upon the cells due to their exposure to the drugs. Both HCC827 rErlo and HCC827 rGefi grow more as distinct clusters, with cells growing on top of each other rather than in a flat monolayer (as HCC827 PTL and HCC827 rAfa do), which could affect the results of the electrical impedance-based xCELLigence assay. In future work, these data should be compared with an alternative technique to measure cell proliferation such as a cell density seeding assay, where growth curves are generated colourmetrically through the quantity of sulforhodamine B dye that binds to the cells and is then solubilised. As all cells are able to take up the dye (regardless of growth

morphology), this assay may more accurately reflect the proliferation rate of HCC827 rErlo and HCC827 rGefi.

Additionally, as demonstrated by the differences when comparing the growth curves of resistant HCC827 and HCC4006 sub lines, decreased growth rate for resistant cells would only benefit some patients; in others, acquired resistance may actually serve to drive growth instead, as is demonstrated by the HCC4006 sub line growth curves.

Interestingly, the HCC4006 parental cell line is not the fastest growing out of the three sub lines, while HCC4006 rGefi grows the fastest. Meanwhile, HCC4006 rErlo and HCC4006 rAfa grow the slowest. This is an indication that while in some cases resistance can slow cell proliferation, in others it can actually increase it. This is likely due to differences in pathway activation/circumvention caused by differing resistance mechanisms between the two parental cell lines (HCC827 and HCC4006). Next-generation sequencing (NGS) alongside bioinformatic analysis would be a useful tool in this context to help elucidate mutations that could be contributing to these differences in growth patterns to be able to compare across cell lines, and should form a part of future work carried out on this project. As all HCC4006 sub lines grew in a monolayer rather than in clusters, these data should represent a more accurate reflection of their growth dynamics when compared to HCC827 sub-lines, although a cell density seeding assay should still be carried out for the sake of comparison and reliability. Additionally, it would be interesting to generate growth curves for the cells when growing without their resistant drug present in the culture conditions to model how tumour cells might grow when a patient is switching treatment regimes and is thus not undergoing therapy for a period of time.

Furthermore, quantifying the differences in cell morphology observed between the parental and resistant cell lines would allow for a preliminary investigation into phenotypic differences. Analysing images of each of the cell lines through a platform such as CellProfiler<sup>51</sup> would allow for high-throughput quantitative examination of various morphological differences such as shape, size and even texture, along with cell grouping/clustering.

#### **4.2. EGFR TKI resistance leads to cross-resistance to paclitaxel treatment in multiple HCC827 and HCC4006 resistant sub-lines**

Resistance to EGFR inhibitors was associated with increased paclitaxel resistance in afatinib-adapted HCC827 cells compared to the parental HCC827 cells. Cross-resistance to paclitaxel was also observed in the erlotinib and afatinib resistant HCC4006 sub-lines but not cells adapted to gefitinib. This extent of cross-resistance was not initially hypothesised, as paclitaxel's most common mechanism of action works by arresting cell division through the inhibition of microtubule destabilisation, which induces mitotic arrest and cell death in a subset of the cellular population<sup>52</sup>. As paclitaxel is not commonly known to engage in the EGFR signalling pathway, the cause of this resistance could be multivariate; for example, a study performed on oral cavity squamous cell carcinoma has shown that paclitaxel treatment significantly reduced EGFR activation<sup>53</sup> and thus in part attenuates the proliferative effects of its signalling pathways, although this does not explain the lack of resistance seen in HCC4006 rGefi. Drug efflux could be another possible cause, as it has been demonstrated that patients with NSCLC can harbour cancer cells with increased expression of ABCB1<sup>54</sup>, an ATP binding cassette strongly implicated in multi-drug resistance<sup>55</sup>. Expression of ABCB1 has also been tied to paclitaxel response in NSCLC, with increased expression resulting

in a lower response rate<sup>54</sup>. Pre-treating cells with verapamil (a phenylalkylamine L-type calcium channel antagonist) can attenuate the effects of drug efflux by decreasing ABCB1 expression in NSCLC<sup>56</sup>, so further work could be undertaken to investigate whether pre-treating the sub-lines that demonstrated paclitaxel resistance with verapamil restores sensitivity to the drug.

#### **4.3. A possible shift to MET signalling may affect the response of resistant HCC827 and HCC4006 cell lines to osimertinib and cabozantinib**

Resistance is seen again in the HCC827 resistant cell lines when treated with the third generation EGFR inhibitor osimertinib, although the extent of resistance seen here is much more significant than it was with paclitaxel. Fold-resistance of 3642, 6523, and 2714 for HCC827 rErlo, HCC827 rGefi and HCC827 rAfa respectively demonstrates that the resistant sub lines are thousands of times more resistant than the parental cells. While not as high as in HCC827, fold-resistance is still high in the HCC4006 resistant sub-lines (1,000, 653, 553 for erlotinib, gefitinib and afatinib resistant cell lines respectively) when compared to the parental cells. As a third generation EGFR TKI, osimertinib was specifically designed and is able to overcome the most prevalent T790M resistance mutation<sup>57</sup>. These data thus suggest that resistance in the case of both HCC827 and HCC4006 sub lines is not due to T790M, but rather to a different factor. After the T790M mutation, the most common known mechanism of resistance in NSCLC treated with EGFR inhibitors is MET amplification, making it the most likely explanation in this scenario. There is significant cross-talk between the EGFR and MET signalling pathways, which allow for common downstream signalling effectors to remain active despite continuous EGFR inhibition. This could explain the over thousand-fold resistance seen in the resistant HCC827 sub lines.

With 4 out of 6 EGFR TKI resistant HCC827 and HCC4006 sub-lines demonstrating enhanced sensitivity to MET inhibitor cabozantinib compared to the parental cells, it appears to be a comparatively effective drug at overcoming EGFR inhibitor-mediated resistance, which further supports the hypothesis that MET amplification may be a possible resistance mechanism in some of the drug-adapted cells.

In order to confirm a possible switch to MET signalling, future work should include c-MET expression examination through qPCR and western blot analysis, and the *MET* gene should be investigated through fluorescent *in situ* hybridisation (FISH) and/or next-generation sequencing (NGS) to ascertain gene amplification/ploidy.

#### **4.4. Sensitivity to MEK inhibition emerges in EGFR TKI resistant HCC827 but not HCC4006 cells**

When treated with trametinib, the two HCC827 sub-lines resistant to first generation EGFR inhibitors (HCC827 rErlo and HCC827 rGefi) show increased sensitivity to the drug (0.46 and 0.52x the IC<sub>50</sub> when compared to the parental cells). This suggests an increase in MAPK pathway dependency in these cell lines, which would explain the increased sensitivity. However, HCC827 rAfa shows an increased IC<sub>50</sub> (1.37x higher than the parental cells), which is comparatively low but may be indicative of a shift to the PI3K pathway over from MAPK signalling, which can mediate acquired resistance in NSCLC as a compensatory mechanism to continue the drive towards survival and proliferation<sup>62</sup>. It would be interesting to confirm whether this is indeed occurring through western blot analysis in any future work that is undertaken. Of further interest is the fact that, despite having an increased IC<sub>50</sub> compared to the parental cells (resistance factors of 7.09, 3.56 and 1.94 for erlotinib, afatinib and gefitinib respectively), even HCC4006 rErlo, which displays the highest IC<sub>50</sub> out of all the

HCC4006 sub-lines at 38.07 nM, still has a lower IC50 than the HCC827 parental cell line (IC50 = 57.15) when treated with trametinib. This suggests that overall, the HCC4006 PTL cells are driven more by MAPK signalling than by the PI3K pathway, whereas the reverse is probably true for HCC827 PTL, although this would again require western blot analysis to confirm. Based on these results then, and with the relative ease of shifting between the two pathways to drive and maintain tumourigenesis in non-small cell lung cancer, a combination therapy of trametinib and a PI3K inhibitor on resistant cells appears a prudent line of inquiry to follow. This combination has been trialled by another group in a preclinical model on EGFR TKI resistant cells, with testing performed both *in vitro* and *in vivo*. Results show that the combination of trametinib and PI3K inhibitor taselelisib is effective in HCC827 and HCC4006 cell lines resistant to both gefitinib and afatinib *in vitro*, and *in vivo* the treatment was able to keep tumour size static for at least 21 days (the end point of the experiment) in a xenograft model using gefitinib resistant cells<sup>40</sup>. It would be interesting to determine whether this combination is also applicable to our resistant cell lines as resistance mechanisms can vary based on the protocol used to generate it, even among the same cell lines treated with identical drugs<sup>63</sup>. Furthermore, the study did not include erlotinib-resistant cells, which would be prudent to include as erlotinib sees widespread clinical use and as demonstrated by our data can have significantly different resistance profiles to gefitinib despite their structural and mechanistic similarity.



#### 4.5. Sensitivity to cabozantinib emerges in resistant HCC827 and HCC4006 cell lines

With over half of the EGFR TKI resistant HCC827 and HCC4006 sub-lines demonstrating enhanced sensitivity to MET inhibitor cabozantinib compared to the parental cells, it appears to be a comparatively effective drug at overcoming EGFR inhibitor-mediated resistance. In the HCC827 sub-lines, sensitivity is demonstrated by the erlotinib and gefitinib resistant cells, with resistance factors of 0.22 and 0.015 respectively. While both show significant sensitivity, HCC827 rGefi shows the highest sensitivity of any cell line treated with any of the drugs. By contrast, however, HCC827 rAfa demonstrated some cross-resistance to cabozantinib treatment with a fold-resistance of 1.46. HCC4006 rAfa and rErlo demonstrated resistance factors of 0.32 and 0.55 respectively. Some sensitivity is also shown in the gefitinib resistant HCC4006 sub-line with an RF of 0.85, although HCC827 rAfa was the only statistically significant result. Once again there appears to be a disparity in the IC<sub>50</sub> of the HCC827 and HCC4006 parental cell lines (2.46 vs 8.09  $\mu$ M respectively), demonstrating that the HCC4006 PTL cells have an IC<sub>50</sub> over 3 times higher than the HCC827 parentals. This difference reflects a probable difference in MET amplification status in HCC827 compared to HCC4006 cells; the data thus suggest that HCC827 have increased MET signalling compared to HCC4006, as even the HCC827 sub-line with the highest IC<sub>50</sub> (HCC827 rAfa) for cabozantinib was less than half the IC<sub>50</sub> for HCC4006 PTL (3.59 vs 8.09  $\mu$ M respectively). HCC827 cells have been experimentally demonstrated to undergo MET amplification as a resistance mechanism in response to EGFR inhibition with first-generation inhibitors<sup>58,59</sup> whereas this was not found in HCC4006 adapted cells<sup>60,61</sup>. Thus, concretely determining whether this difference is due to differential MET amplification or due to differences in

expression of other NSCLC oncogenic drivers such as VEGFR, ROS, RET and AXL (which cabozantinib also targets)<sup>36</sup> through qPCR and/or western blotting experiments for example, would be of strong interest.

#### **4.6. EGFR TKI resistant cell lines show no increased sensitivity to dichloroacetate**

Contrary to predictions, there was not one single case of enhanced sensitivity to dichloroacetate treatment in any of the HCC827 or HCC4006 drug-adapted cell lines. It was hypothesised that the increased rates of glycolysis<sup>44</sup> and autophagy<sup>47</sup> seen in resistant cells would result in increased dichloroacetate effectiveness in these sub-lines – instead, it appears that there is no significant difference between the parental and resistant cells (HCC827 rGefi, HCC827 rAfa) or, even more surprisingly, cross-resistance (HCC827 rErlo, HCC4006 rErlo, HCC4006 rGefi, HCC4006 rAfa). One factor that could influence this stark difference is the lack of a tumour micro-environment in the *in vitro* model; one study found that increased glycolysis in EGFR TKI resistant cells only actually mediated resistance through the cancer-associated fibroblasts (CAF)<sup>44</sup>, which explains why a glycolytic inhibitor was only effective in the *in vivo* experiments and not *in vitro*.

In the context of autophagy, it could be that it has decreased in some of the resistant cell lines due to increased activation of the PI3K pathway compared to MAPK, specifically in the context of the trametinib cross-resistance found in the drug-adapted HCC4006 sub-lines. This would need to be experimentally demonstrated however, and if upregulation of the PI3K pathway is indeed occurring in the resistant sub-lines, then a combination assay of a PI3K inhibitor such as taselisib with dichloroacetate may yield an interesting result due to the potential synergy of PI3K inhibition coupled with the

targeting of the resulting increase in autophagy by dichloroacetate. However, increased PI3K activity would still not satisfactorily explain the observed cross-resistance to DCA in the HCC4006 resistant sub-lines due to the discrepancy between dichloroacetate and trametinib cross-resistance; While the IC50s of HCC4006 rErlo and HCC4006 rGefi are near-identical when treated with dichloroacetate, there is a significant difference between their IC50s when treated with trametinib (38.07 vs 10.41 nM respectively). This suggests that there are additional mechanisms at play, although a sparsity of literature on this topic makes it difficult to suggest further possible causes.

#### **4.7. Future work**

As mentioned throughout the discussion, it would be prudent to establish cell signalling profiles (both baseline signalling and signalling when treated with the various drugs) of relevant proteins such as MET, MEK, PI3K and EGFR in all NSCLC sub-lines through western blotting. This would serve to support the hypotheses generated by this data, whilst also serving as a good starting point for exploring effective drug combinations for future dose-response cell viability assays.

As a further part of the characterisation process, it would also be beneficial to generate a cell cycle profile for each of the sub-lines through flow cytometry (using propidium iodide or Hoechst 33342 staining for example) in order to determine whether there is a significant difference in cell cycle progression between the parental and resistant cells. This data could be used to determine whether cell-cycle or checkpoint inhibitors could have potential to overcome resistance in the drug-adapted cell lines.

In order to further elucidate the effects of the drugs on the panel on the cell lines used, annexin V staining could be undertaken to determine the proportion of apoptotic cells after treatment with each of the drugs. This would allow the determination of whether the drugs' effects are cytostatic or cytotoxic for each of the different cell lines and would thus be a useful addition to the characterisation process.

Furthermore, it would be interesting to determine whether a significant side population (SP), characterised by cancer cells with stem-like properties and show resistance to multiple chemotherapeutic drugs<sup>64</sup> is present in any of the cell lines. Side populations display an increased expression of ABCG2 efflux pumps, and their presence can be determined within a general population of cancer cells through staining with Hoechst 33342 or DyeCycle Violet fluorescent dyes using a flow cytometer; SP cells will efflux the dyes through their ABCG2 efflux pumps, whereas non-SP cells will retain the dye inside the cell<sup>64</sup>. If a side-population is indeed present in any of the resistant cell lines then it may provide a further explanation for possible resistance mechanisms.

Side population analysis could further be complimented with NGS (for example whole exome sequencing) followed by bioinformatic analysis of clones from the parental and resistant cell lines to determine the acquisition of mutations after being exposed to their respective drugs. This would help to build a more complete profile of the cell lines as well as identifying potential new biomarkers of resistance and/or sensitivity for each cell line. This information could then be further extended with the addition of deep amplicon sequencing, allowing rare compound mutations to be identified<sup>65</sup> as well as determining whether there was a resistant sub-population already present in the parental cells.

#### 4.8. Conclusions

To conclude, the characterisation process of the EGFR TKI resistant non-small cell lung cancer cell lines HCC827 and HCC4006 demonstrated a high extent of cross-resistance to the drugs selected for the panel. Significant cross-resistance was observed in all HCC827 resistance cell lines when treated with paclitaxel and in HCC4006 rErlo and HCC4006 rAfa, along with several thousand and hundred-fold resistance in the HCC827 and HCC4006 resistant cell lines respectively when treated with third-generation EGFR inhibitor osimertinib. Trametinib demonstrated some effectiveness in overcoming resistance in HCC827 cells, while HCC827 cells resistant to first-generation EGFR inhibitors demonstrated significant sensitivity when treated with cabozantinib, and there was also some sensitivity seen in HCC4006 sub-lines, although the difference between the parental cell line and the cell lines resistant to first generation inhibitors was not statistically significant. Somewhat surprisingly, dichloroacetate showed either no significant difference in the resistant cell lines compared to the parentals (HCC827 rGefi, HCC827 rAfa) or cross resistance (HCC827 rErlo, all HCC4006 resistant sub-lines). The results obtained also highlight the persistent heterogeneity presence in the context of acquired drug resistance in cancer; despite being derived from the same cancer type and containing very similar EGFR-activating mutations, they demonstrate very different responses between equivalent HCC827 and HCC4006 sub-lines when treated with the same drugs. This makes it hard to pin down any particularly effective therapy from the drug panel screening; what works well on one HCC827 sub-line to overcome resistance may have the opposite effect on the equivalent HCC4006 sub-line (for example as occurred with trametinib treatment). Based on the observed data, however, it appears that cabozantinib is the most effective of the tested therapies,

with significant therapeutic potential in some resistant cell lines (HCC827 rGefi, HCC827 rErlo and HCC4006 rAfa). The next stage would be to determine its efficacy in an *in vivo* model so see whether the results generated in this *in vitro* model would translate into clinically-relevant data in a complete tumour environment.

Even when drug screening projects such as this do not demonstrate immediate potential for clinically actionable results due to wide-ranging heterogeneity, continued characterisation efforts of drug-resistant cell lines from the RCCL nonetheless remains important. For example, it allows other researchers using cells from the RCCL to have a more complete understanding of how the cells react to different treatments and conditions, and allows them to take this into account when designing their experiments. Additionally, laboratory work coupled with bioinformatic genomic analysis allows potential new biomarkers of drug resistance/sensitivity to be uncovered which can then be used in various ways, from improved patient stratification to applications in personalised medicine.

## Bibliography

1. Cancer Research UK. 2019
2. Hanahan, D. & Weinberg, R. A. The Hallmarks of Cancer. *Cell* **100**, 57–70 (2000).
3. Bailey, M. H. *et al.* Comprehensive Characterization of Cancer Driver Genes and Mutations. *Cell* **173**, 371–385.e18 (2018).
4. Cancer Treatment Centers of America. Lung cancer stages.
5. Faguet, G. B. Chemotherapy drugs. *The War on Cancer* 69–83 (2008). doi:10.1007/978-1-4020-3617-0\_6
6. ASTOLFI, L. *et al.* Correlation of adverse effects of cisplatin administration in patients affected by solid tumours: A retrospective evaluation. *Oncol. Rep.* **29**, 1285–1292 (2013).
7. Kanellakis, N. I., Jacinto, T. & Psallidas, I. Targeted therapies for lung cancer: how did the game begin? *Breathe* **12**, 177–179 (2016).
8. Cohen, M. H. FDA Drug Approval Summary: Erlotinib (Tarceva(R)) Tablets. *Oncologist* **10**, 461–466 (2005).
9. Wieduwilt M. J. & Moasser M. M. The epidermal growth factor receptor family: Biology driving targeted therapeutics. *Cell Mol Life Sci* **65**, 1566–1584 (2011).
10. Riely, G. J. *et al.* Clinical course of patients with non-small cell lung cancer and epidermal growth factor receptor exon 19 and exon 21 mutations treated with gefitinib or erlotinib. *Clin. Cancer Res.* **12**, 839–844 (2006).
11. Gadzar, A. F. Activating and resistance mutations of EGFR in non-small cell lung cancer: role in clinical response to EGFR tyrosine kinase inhibitors. *Oncogene* **28**, 1–14 (2010).
12. Carey, K. D. *et al.* Kinetic analysis of epidermal growth factor receptor somatic mutant proteins shows increased sensitivity to the epidermal growth factor receptor tyrosine kinase inhibitor, erlotinib. *Cancer Res.* **66**, 8163–8171 (2006).
13. Schiller, J. H. *et al.* Comparison of Four Chemotherapy Regimens for Advanced Non-Small-Cell Lung Cancer. *N. Engl. J. Med.* **346**, 92–98 (2002).
14. Housman, G. *et al.* Drug resistance in cancer: an overview. *Cancers (Basel)*. **6**, 1769–92 (2014).
15. Corrà, F., Agnoletto, C., Minotti, L., Baldassari, F. & Volinia, S. The Network of Non-coding RNAs in Cancer Drug Resistance. *Front. Oncol.* **8**, 327 (2018).
16. Sequist, L. V *et al.* Nihms298935.Pdf. **3**, (2011).
17. COSMIC - Mutation COSV51765492. Available at: <https://cancer.sanger.ac.uk/cosmic/mutation/overview?id=86748373>. (Accessed: 28th January 2020)
18. Westover, D., Zugazagoitia, J., Cho, B. C., Lovly, C. M. & Paz-Ares, L. Mechanisms of acquired resistance to first-and second-generation EGFR tyrosine kinase inhibitors. *Ann. Oncol.* **29**, i10–i19 (2018).
19. Sos, M. L. *et al.* Chemogenomic profiling provides insights into the limited activity of irreversible EGFR inhibitors in tumor cells expressing the T790M EGFR resistance

- mutation. *Cancer Res.* **70**, 868–874 (2010).
20. Yun, C.-H. *et al.* The T790M mutation in EGFR kinase causes drug resistance by increasing the affinity for ATP. *Proc. Natl. Acad. Sci.* **105**, 2070–2075 (2008).
  21. Kim, Y. *et al.* The EGFR T790M Mutation in Acquired Resistance to an Irreversible Second-Generation EGFR Inhibitor. *Mol. Cancer Ther.* **11**, 784–791 (2012).
  22. Furuyama, K. *et al.* Sensitivity and kinase activity of epidermal growth factor receptor (EGFR) exon 19 and others to EGFR-tyrosine kinase inhibitors. *Cancer Sci.* **104**, 584–589 (2013).
  23. Miller, V. A. *et al.* Afatinib versus placebo for patients with advanced, metastatic non-small-cell lung cancer after failure of erlotinib, gefitinib, or both, and one or two lines of chemotherapy (LUX-Lung 1): A phase 2b/3 randomised trial. *Lancet Oncol.* **13**, 528–538 (2012).
  24. Deeks, E. D. & Keating, G. M. Afatinib in advanced NSCLC: a profile of its use. *Drugs Ther. Perspect.* **34**, 89–98 (2018).
  25. Wu, Y. L. *et al.* Dacomitinib versus gefitinib as first-line treatment for patients with EGFR-mutation-positive non-small-cell lung cancer (ARCHER 1050): a randomised, open-label, phase 3 trial. *Lancet Oncol.* **18**, 1454–1466 (2017).
  26. Cross, D. A. E. *et al.* AZD9291, an irreversible EGFR TKI, overcomes T790M-mediated resistance to EGFR inhibitors in lung cancer. *Cancer Discov.* **4**, 1046–1061 (2014).
  27. Mok, T. S. *et al.* Osimertinib or Platinum–Pemetrexed in EGFR T790M–Positive Lung Cancer. *N. Engl. J. Med.* **376**, 629–640 (2017).
  28. Soria, J.-C. *et al.* Osimertinib in Untreated EGFR -Mutated Advanced Non–Small-Cell Lung Cancer. *N. Engl. J. Med.* **378**, 113–125 (2018).
  29. COSMIC - Mutation COSV51766493. Available at: <https://cancer.sanger.ac.uk/cosmic/mutation/overview?id=86749152>. (Accessed: 28th January 2020)
  30. Tan, C. S., Cho, B. C. & Soo, R. A. Next-generation epidermal growth factor receptor tyrosine kinase inhibitors in epidermal growth factor receptor -mutant non-small cell lung cancer. *Lung Cancer* **93**, 59–68 (2016).
  31. Dry, J. R. *et al.* Acquired Resistance to the Mutant-Selective EGFR Inhibitor AZD9291 Is Associated with Increased Dependence on RAS Signaling in Preclinical Models. *Cancer Res.* **75**, 2489–2500 (2015).
  32. Engelman, J. A. *et al.* MET Amplification Leads to Gefitinib Resistance in Lung Cancer by Activating ERBB3 Signaling. *Science (80-. ).* **316**, 1039–1043 (2007).
  33. Mughal, A., Aslam, H. M., Sheikh, A., Khan, A. M. H. & Saleem, S. c-Met inhibitors. *Infect. Agent. Cancer* **8**, 13 (2013).
  34. Underiner, T. L., Herbertz, T. & Miknyoczki, S. J. Discovery of small molecule c-Met inhibitors: Evolution and profiles of clinical candidates. *Anticancer. Agents Med. Chem.* **10**, 7–27 (2010).
  35. Rehman, S. & Dy, G. K. MET Inhibition in Non-Small Cell Lung Cancer. 100–111 (2019).
  36. Neal, J. W. *et al.* Erlotinib, cabozantinib, or erlotinib plus cabozantinib as second-line or third-line treatment of patients with EGFR wild-type advanced non-small-cell lung cancer (ECOG-ACRIN 1512): a randomised, controlled, open-label, multicentre, phase 2



- trial. *Lancet Oncol.* **17**, 1661–1671 (2016).
37. Reckamp, K. L. *et al.* Phase II Trial of Cabozantinib Plus Erlotinib in Patients With Advanced Epidermal Growth Factor Receptor (EGFR)-Mutant Non-small Cell Lung Cancer With Progressive Disease on Epidermal Growth Factor Receptor Tyrosine Kinase Inhibitor Therapy: A California. *Front. Oncol.* **9**, 132 (2019).
  38. NICE. TRAMETINIB. *National Institute of Health and Care Excellence*
  39. Tricker, E. M. *et al.* Combined EGFR/MEK Inhibition Prevents the Emergence of Resistance in EGFR-Mutant Lung Cancer. *Cancer Discov.* **5**, 960–971 (2015).
  40. Sato, H. *et al.* Combined inhibition of MEK and PI3K pathways overcomes acquired resistance to EGFR-TKIs in non-small cell lung cancer. *Cancer Sci.* **109**, 3183–3196 (2018).
  41. Chiang, C.-T. *et al.* mTORC2 contributes to the metabolic reprogramming in EGFR tyrosine-kinase inhibitor resistant cells in non-small cell lung cancer. *Cancer Lett.* **434**, 152–159 (2018).
  42. Michelakis, E. D., Webster, L. & Mackey, J. R. Dichloroacetate (DCA) as a potential metabolic-targeting therapy for cancer. *Br. J. Cancer* **99**, 989–94 (2008).
  43. Tan Allen, K. *et al.* Dichloroacetate alters Warburg metabolism, inhibits cell growth, and increases the X-ray sensitivity of human A549 and H1299 NSC lung cancer cells. *Free Radic. Biol. Med.* **89**, 263–273 (2015).
  44. Apicella, M. *et al.* Increased Lactate Secretion by Cancer Cells Sustains Non-cell-autonomous Adaptive Resistance to MET and EGFR Targeted Therapies. *Cell Metab.* **28**, 848-865.e6 (2018).
  45. Lu, X. *et al.* Dichloroacetate enhances the antitumor efficacy of chemotherapeutic agents via inhibiting autophagy in non-small-cell lung cancer. *Cancer Manag. Res.* **Volume 10**, 1231–1241 (2018).
  46. White, E. The role for autophagy in cancer. *J. Clin. Invest.* **125**, 42–46 (2015).
  47. Han, W. *et al.* EGFR Tyrosine Kinase Inhibitors Activate Autophagy as a Cytoprotective Response in Human Lung Cancer Cells. *PLoS One* **6**, e18691 (2011).
  48. Michaelis, M., Wass, M. N. & Cinatl, J. Drug-adapted cancer cell lines as preclinical models of acquired resistance. *Cancer Drug Resist.* (2019). doi:10.20517/cdr.2019.005
  49. ATCC. HCC827. (2016).
  50. ATCC. HCC4006. (2016).
  51. Carpenter, A.E., Jones, T.R., Lamprecht, M. R. *et al.* CellProfiler: image analysis software for identifying and quantifying cell phenotypes. *Genome Biol.* **7**, (2006).
  52. Weaver, B. A. How Taxol/paclitaxel kills cancer cells. *Mol. Biol. Cell* **25**, 2677–81 (2014).
  53. HU, J., ZHANG, N., WANG, R., HUANG, F. & LI, G. Paclitaxel induces apoptosis and reduces proliferation by targeting epidermal growth factor receptor signaling pathway in oral cavity squamous cell carcinoma. *Oncol. Lett.* **10**, 2378–2384 (2015).
  54. Chiou, J. F. *et al.* Comparing the relationship of Taxol-based chemotherapy response with P-glycoprotein and lung resistance-related protein expression in non-small cell lung cancer. *Lung* **181**, 267–73 (2003).
  55. Juliano, R. L. & Ling, V. A surface glycoprotein modulating drug permeability in Chinese

- hamster ovary cell mutants. *Biochim. Biophys. Acta - Biomembr.* **455**, 152–162 (1976).
56. Wang, J. *et al.* Down-regulation of P-glycoprotein is associated with resistance to cisplatin and VP-16 in human lung cancer cell lines. *Anticancer Res.* **30**, 3593–8 (2010).
  57. Ahn, M. *et al.* Osimertinib in patients with T790M mutation-positive, advanced non-small cell lung cancer: Long-term follow-up from a pooled analysis of 2 phase 2 studies. *Cancer* **125**, 892–901 (2019).
  58. Suda, K. *et al.* Reciprocal and Complementary Role of MET Amplification and EGFR T790M Mutation in Acquired Resistance to Kinase Inhibitors in Lung Cancer. *Clin. Cancer Res.* **16**, 5489–5498 (2010).
  59. Cappuzzo, F. *et al.* MET increased gene copy number and primary resistance to gefitinib therapy in non-small-cell lung cancer patients. *Ann. Oncol.* **20**, 298–304 (2008).
  60. Ware, K. E. *et al.* A mechanism of resistance to gefitinib mediated by cellular reprogramming and the acquisition of an FGF2-FGFR1 autocrine growth loop. *Oncogenesis* **2**, e39-9 (2013).
  61. Wu, S.-G. *et al.* IGFBP7 Drives Resistance to Epidermal Growth Factor Receptor Tyrosine Kinase Inhibition in Lung Cancer. *Cancers (Basel)*. **11**, (2019).
  62. Ciuffreda, L. *et al.* Signaling Intermediates (MAPK and PI3K) as Therapeutic Targets in NSCLC. *Curr. Pharm. Des.* **20**, 3944–3957 (2014).
  63. Shien, K. *et al.* Acquired Resistance to EGFR Inhibitors Is Associated with a Manifestation of Stem Cell-like Properties in Cancer Cells. *Cancer Res.* **73**, 3051–3061 (2013).
  64. Ho, M. M., Ng, A. V., Lam, S. & Hung, J. Y. Side Population in Human Lung Cancer Cell Lines and Tumors Is Enriched with Stem-like Cancer Cells. *Cancer Res.* **67**, 4827–4833 (2007).
  65. Namba, K. *et al.* Application of amplicon-based targeted sequencing with the molecular barcoding system to detect uncommon minor EGFR mutations in patients with treatment-naïve lung adenocarcinoma. *BMC Cancer* **19**, 175 (2019).